OPTIMIZATION OF OVER-EXPRESSION AND PURIFICATION OF HUMAN LEUKOTRIENE C4 SYNTHASE MUTANT R104A FOR STRUCTURE-FUNCTION STUDIES BY TWO-DIMENSIONAL CRYSTALLIZATION AND ELECTRON CRYSTALLOGRAPHY

A Thesis
Presented to
The Academic Faculty

by

Laura Yaunhee Kim

In Partial Fulfillment
of the Requirements for the Degree
Master of Science in the
School of Biology

Georgia Institute of Technology
December 2012

OPTIMIZATION OF OVER-EXPRESSION AND PURIFICATION OF HUMAN LEUKOTRIENE C4 SYNTHASE MUTANT R104A FOR STRUCTURE-FUNCTION STUDIES BY TWO-DIMENSIONAL CRYSTALLIZATION AND ELECTRON CRYSTALLOGRAPHY

Approved by:

Dr. Ingeborg Schmidt-Krey, Advisor
School of Biology
School of Chemistry and Biochemistry
Georgia Institute of Technology

Dr. Thomas DiChristina
School of Biology
Georgia Institute of Technology

Dr. Raquel L. Lieberman
School of Chemistry and Biochemistry
Georgia Institute of Technology

Date Approved: July 24, 2012

I dedicate this work to my father Sun Dong Kim, mother In Ok Kim, and sister Esther Kim, who have supported me from the very beginning. This work could not have been completed without your love and encouragement.

ACKNOWLEDGEMENTS

I would like to thank my advisor, Dr. Inga Schmidt-Krey, for guiding and supporting me throughout my academic studies. I would like to thank her for her consistent availability and scientific input during every step of research. Without her guidance this work would not have been possible.

I am in debt to my family and friends for their unflinching support and encouragement, without which none of this would be possible.

I am also very grateful to all the Schmidt-Krey lab members, especially Matthew Johnson and Maureen Metcalfe, for their support and input into this work.

Finally, I am thankful towards my thesis committee members, Dr. Raquel Lieberman and Dr. Thomas DiChristina for their feedback and suggestions in this work.

TABLE OF CONTENTS

LIST OF TABLES

LIST OF FIGURES

LIST OF SYMBOLS AND ABBREVIATIONS

PDB	Protein Data Bank
$hLTC_4S$	Human Leukotriene C_4 Synthase
MP	Membrane Protein
LT	Leukotriene
LTA_4	Leukotriene A_4
GSH	Reduced glutathione
IMAC	Immobilized metal affinity chromatography
2D	Two-dimensional
3D	Three-dimensional
LPR	Lipid-to-Protein ratio
WT	Wild-type
AA	Arachadonic acid
5-LO	5-lipoxygenase
FLAP	5-lipoxygenase activating protein
MAPKK	Map kinase kinase
5-HPETE	5-hydroperoxyeicosatetraenoic acid
5-HETE	5-hydroxyeicosatetraenoic acid
GPCR	G-protein coupled receptor
MRP1	Multidrug resistant protein 1
MGST	Microsomal glutathione *S*-transferase
SDS	Sodium dodecyl sulfate

PAGE	Polyacrylamide gel electrophoresis
CMC	Critical micelle concentration
CMT	Critical micelle temperature
MWCO	Molecular weight cutoff
MAPEG	Membrane-associated proteins in prostaglandin and eicosanoid metabolism

SUMMARY

Membrane proteins (MPs) are macromolecular structures involved in a number of diverse cellular functions, from energy conversion and signal transduction, to ion transport across the phospholipid bilayer. MPs represent a large number of drug targets and due to their localization within a lipid bilayer, their over-expression, purification and crystallization embody significant hurdles to three-dimensional structure determination, which is essential for rational drug design. The difficulties associated with MP structure determination relate to why the availability of their three-dimensional (3D) structures is severely underrepresented in the Protein Data Bank (PDB) when compared to that of soluble proteins. Structural determination of membrane proteins answers critical questions related to their structure-function relationship and represents an intensely studied field in biology.

Human leukotriene C_4 synthase ($hLTC_4S$) is an integral MP involved in the 5-lipoxygenase pathway. $hLTC_4S$ catalyzes the conjugation of leukotriene A_4 (LTA_4) and reduced glutathione (GSH) to produce product leukotriene C_4 (LTC_4), which along with its metabolites leukotriene D_4 (LTD_4) and leukotriene E_4 (LTE_4) represent the cysteinyl leukotrienes that mediate pro-inflammatory activities such as asthma and bronchoconstriction. Alongside wild-type (WT) enzyme, mutant construct R104A was studied, an amino acid side chain implicated in substrate binding. Under the mentorship of Dr. Ingeborg Schmidt-Krey and collaboration with graduate student Matthew C. Johnson, I have been able to reproduce the over-expression, purification and two-dimensional (2D) crystallization of $hLTC_4S$ based on previously published protocols (Schmidt-Krey *et al*., 2004 and Zhao *et al*., 2010), with slight modifications. Using these methods, preliminary 2D crystals of the R104A mutant enzyme have been grown, representing progress in the purification of $hLTC_4S$ for two-dimensional crystallization

by electron crystallography. 2D crystallization trials investigating the optimal conditions to grow large, well-ordered 2D crystals of the mutant enzyme via dialysis were investigated, primarily by varying the time in dialysis and lipid-to-protein ratio (LPR), with a focus on lower LPRs. In total, this work displays an adjusted protocol for the purification of $hLTC_4S$ and preliminary examinations of conditions for 2D crystallization with the final goal of visualizing conformational changes of $hLTC_4S$ WT and mutant R104A.

CHAPTER 1

1. OVER-EXPRESSION OF HUMAN LEUKOTRIENE C_4 SYNTHASE IN SCHIZOSACCHAROMYCES POMBE

1.1 BACKGROUND AND SIGNIFICANCE

Membrane protein overview

Membrane proteins (MPs) are specialized macromolecules localized within the lipid bilayer that oftentimes aid in the communication between both sides of the membranes environment. MPs are involved in numerous cellular functions, including signal transduction, small molecule translocation, and energy conversion (Krebs *et al*., 2003; Appel *et al*., 2009; Morosinotto *et al*., 2006) and encode for up to 30% of proteins of the eukaryotic genome. With their in-depth involvement in cellular processes and large representation in the human genome, MP malfunction can play a critical role in several disease pathologies and represent ~60% of drug targets (Drews, 2000 and Cooper, 2004 Lappano and Maggiolini, 2011). Despite their importance in cell physiology, available crystal structures of MPs are severely underrepresented when compared to their soluble counterparts, with less than 0.5% of the total structures deposited in the Protein Data Bank (PDB) representative of MPs (Kühlbrandt, 2012). High-resolution structure determination of MPs is critical for rational drug design and to better understand the basis and mechanism of protein-lipid and protein-protein interactions within the phospholipid bilayer. In order to successfully solve the 3D structure of any MP, several technical difficulties must be overcome, including their over-expression, purification, and crystallization (Renault *et al*., 2006).

Difficulties encountered during membrane protein over-expression

The extensive and comprehensive functional and structural study of a MP requires large amounts of homogenous, pure and biologically active protein. The first hurdle that

must be overcome is their over-expression within an expression system. Relying on naturally expressed protein is problematic since most MPs are expressed *in vivo* at insufficiently low concentrations (Grishammer and Tate, 1995, Hays *et al*., 2010). An example of an MP successfully over-expressed in its native tissue is bacteriorhodopsin, which is the only protein present in the Halobacterium halobium purple membrane (Oesterhelt and Stoeckenius, 1974). Naturally expressed proteins cannot be manipulated by genetic modifications such as affinity tagging, to assist in detection and purification, and point mutations, to study effects of changes in amino acid sequence on tertiary structure. Thus, researchers need to rely on the homologous or heterologous over-expression of recombinant membrane proteins, often within a prokaryotic bacterial or eukaryotic yeast expression system such as *Escherichia coli* (*E. coli*) or *Saccharomyces cerevisiae* (*S. cerevisiae*), respectively (Wagner *et al*., 2006).

MP over-expression is organized into two parts: first, the transcription and translation of genetic material, and second, membrane insertion and folding (Kozak, 1991, Kozak 1992, Grishammer and Tate, 1995). There are factors that influence the expression of membrane proteins. A study of 1092 predicted soluble and MPs expressed in *S. cerevisiae* showed that smaller proteins (less than 60 kDa), with a lower number of transmembrane segments (less that 5 transmembrane segments), and a high percentage of hydrophobic residues found in transmembrane segments (more than 70%) were highly expressed (White *et al*., 2007). On the other hand, another study of 601 inner membrane proteins expressed in *E. coli* showed conflicting data: expression levels are not related to superficial sequence characteristics such as codon usage protein size, hydrophobicity and the number of transmembrane helices, leading to the conclusion that expression levels cannot be easily predicted (Daley *et al*., 2005).

Inducible expression is preferred to constitutive expression as it allows regulated control of promoter activity, which in turn controls levels of recombinant protein expression (Abeyrathne *et al*., 2010). MP over-expression is often toxic to the cell,

leading to the production of inactive protein or insoluble aggregates (Miroux and Walker, 1996) and decreasing host-cell sustainability. Also, high expression levels may apply metabolic expenditures on the host cell, such as overloading the Sec translocon machinery that may cause a decrease in growth rates (Kumar and Singh, 2006 and Wagner *et al*., 2007).

Prokaryotic and eukaryotic gene expression differs in many ways, which should be considered to optimize functional protein production. In this work $hLTC_4S$ was expressed in the fission yeast *Schizosaccharomyces pombe*. A major difference between prokaryotic and eukaryotic MP expression is where over-expression will occur. In bacteria, over-expression occurs in the cytoplasmic membrane whereas in eukaryotes it occurs in the endoplasmic reticulum. Eukaryotic expression systems may be preferred over prokaryotic: polypeptide elongation and protein folding rates are greater in prokaryotes, leading to the possibility of mistargeting and misfolding during expression (Wagner *et al.,* 2006). Upon insertion into the membrane, the polypeptide must undergo proper folding in order to obtain its final and enzymatically active 3D conformation. The choice between a eukaryotic or prokaryotic expression host is critical, as certain membrane proteins require specific phospholipid composition for activity (Grishammer and Tate, 1995). For example, the sodium- and chloride- dependent aminobutyric acid (GABA) transporter (Shouffani and Kanner, 1990) and serotonin transporter (SERT) (Tate, 2001) both require cholesterol for activity, and so should be expressed in a eukaryotic expression system and not in *E. coli* which does not contain cholesterol in its native cell membrane. However, the addition of necessary lipids during and/or after purification can restore functionality, as was seen for LacY where translocation across the *E. coli* inner membrane was restored upon addition of phosphatidylethanolamine (PE), a non-protein molecular chaperone (Bogdanov *et al*., 1999). Similarly, the expression of MPs that require post-translational modifications for activity, such as glycosylation or phosphorylation, should be handled in eukaryotic expression hosts

because bacterial cells are unable to modify proteins after translation (Abeyrathne *et al.,* 2010).

When considering eukaryotic expression systems, yeasts are cheaper and easier to care for when compared to other eukaryotic expression systems like insect and mammalian cells (Abeyrathne *et al*., 2010). The most commonly used species of yeast include *Saccharomyces cerevisiae* (*S. cerevisiae*), *Schizosaccharomyces pombe* (*S. pombe*), and *Pischia pastoris* (*P. pastoris*). As mentioned earlier, $hLTC_4S$ was expressed in *S. pombe* (Schmidt-Krey *et al*., 2004). Although budding yeast *S. cerevisiae* is more frequently used as a host for protein expression investigations, *S. pombe* has been employed for the successful over-expression of several integral MPs, including human glucose transporters GLUT1, GLUT2, and GLUT 3 (Yang *et al*., 2009) and human chemokine receptor CCR-5 (Chen *et al*., 2011). In another study, it was shown that fission yeast *S. pombe* expressed more protein than *S. cerevisiae*: Sander *et al*. found that the human D_{2S} dopamine receptor could be expressed at greater concentrations in *S. pombe* (Sander *et al*., 1994). Furthermore, *S. pombe*'s transcription initiation is similar to that of higher eukaryotes (Bharathi *et al*., 1997). A notable disadvantage of yeast expression is the presence of endogenous proteases in vacuoles that can affect protein production (Jones, 2002). Several MP structures have been determined using yeast expression systems: single particle analysis and 2D crystallization of voltage-sensitive K^+- channel (Parcej and Eckhardt-Strelau, 2002), x-ray crystallography of monoamine oxidase-B (Binda *et al*., 2003), and x-ray crystallography of yeast aquaporin Aqy1 (Fischer *et al.,* 2009).

If the quality of expressed MPs is sub-par, i.e. heterogeneous due to proteolytic cleavage or posttranslational modifications, it is important to address these issues as they will affect crystallization trials negatively. For heterogeneity due to proteolysis, flexible domains of the enzyme should be removed, which can be recognized by first identifying the proteolytically stable core by mild proteolytic treatment in conjunction with mass

spectrometry. A refined DNA construct was built for the *E. coli* glycerol-3-phosphate transporter, GlpT (Auer *et al*., 2001) white full-length KcsA K^+-channel was treated with proteases trypsin, chymotrypsin, and subtilisin to reveal the proteolytically resistant core used for crystallization trials (Cohen and Chait, 2001). Upon successful over-expression, proper insertion and folding should be confirmed by testing the activity of the protein. Ideally, the host cell should not express any endogenous proteins with similar activity as the MP of interest and any naturally expressed protein should not interfere with the activity measurement of the MP of interest (Abeyrathne *et al*., 2010).

Membrane Protein of Interest: Leukotriene C_4 Synthase

Leukotriene C_4 Synthase (LTC_4S) is an 18 kDa, 150 amino acid, integral MP localized to the outer membrane of mast cells, eosinophils, basophils, endothelial cells and platelets (Christmas *et al*., 2002 and Strid *et al*., 2009). LTC_4S is encoded by *LTC4S*, a 2.5 kb gene with chromosomal location on 5q35 (Penrose et al., 1996). LTC_4S is a lyase that catalyzes the conjugation of leukotriene A_4 (LTA_4) and reduced glutathione (GSH) to yield leukotriene C_4 (LTC_4) (Figure 1.1) (Yoshimoto *et al., 1988,* Nicholson *et al.,* 1993). LTC_4S activity is amplified by Mg^{+2} and decreased by Co^{+2} ions (Nicholson *et al*., 1992).

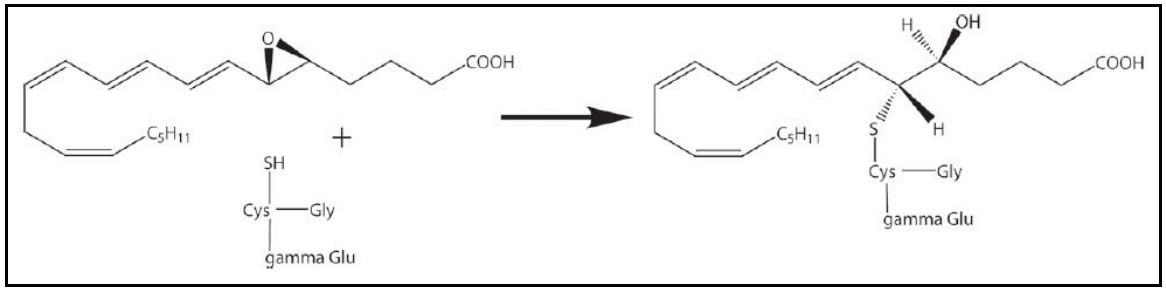

Figure 1.1. Schematic of LTC_4S enzymatic reaction. LTC_4S is responsible for conjugating substrates leukotriene A_4 (top left) and reduced glutathione (bottom left) to form leukotriene C_4 (right) in a non-reversible enzymatic reaction (Molina *et al*., 2007).

LTC_4 and its metabolites LTD_4 and LTE_4 are the cysteinyl leukotrienes produced from the conversion of arachidonic acid in a multistep enzyme pathway called the 5-lipoxygenase pathway. The 5-lipoxygenase pathway mediates asthmatic airway inflammation and bronchoconstriction and is active in leukocytes like neutrophils, mast cells and monocytes (Duroudier *et al*., 2009). As seen in Figure 1.2 (Soberman and Christmas, 2003), this enzymatic reaction occurs in several distinct steps: leukocytes are activated causing a rise in free calcium which induces the translocation of calcium-dependent cytoplasmic phospholipase A_2 ($cPLA_2$) to the nuclear envelope where it releases arachidonic acid (AA) (Glover *et al.,* 1995). Next, 5- lipoxygenase (5-LO) is phosphorylated by MAP kinase kinase (MAPKK) and translocates through the nuclear pore, associates with 5-lipoxygenase activating protein (FLAP) (Rouzer and Kargman, 1988, Kargman *et al.,* 1992). FLAP then presents AA to 5-LO, the rate-limiting enzyme, which then oxygenates AA to form the unstable intermediate 5-hydroperoxyeicosatetraenoic acid (5-HPETE). 5-HPETE is either hydrolysed to form 5-hydroxyeicosatetraenoic acid (5-HETE) or converted to the unstable epoxide, leukotriene A_4 (LTA_4), by dehydration (Rouzer *et al.,* 1986). LTA_4 can either form LTB_4 via LTA_4 hydrolase (Radmark *et al.,* 1988), or form LTC_4 via LTC_4 synthase (LTC_4S). LTC_4 is then transported out of the cell by multidrug resistance protein 1 (MPR1) (Lam *et al.,* 1989, Jedlitschky *et al.,* 1994, Loe *et al.,* 1996), where it is hydrolyzed by peptidases to form metabolites LTD_4 and LTE_4, which bind G protein-coupled receptors (GPCRs) $CysLT_1$ or $CysLT_2$, causing smooth muscle constriction and inflammation (Lewis *et al.,* 1990, Samuelsson *et al.,* 1987, Taylor *et al.,* 1989). The $CysLT_1$ receptor has higher binding affinity for LTD_4, while $CysLT_2$ receptor has high binding affinity for LTC_4 and LTD_4 (Lynch *et al.,* 1999, Hui *et al.,* 2001).

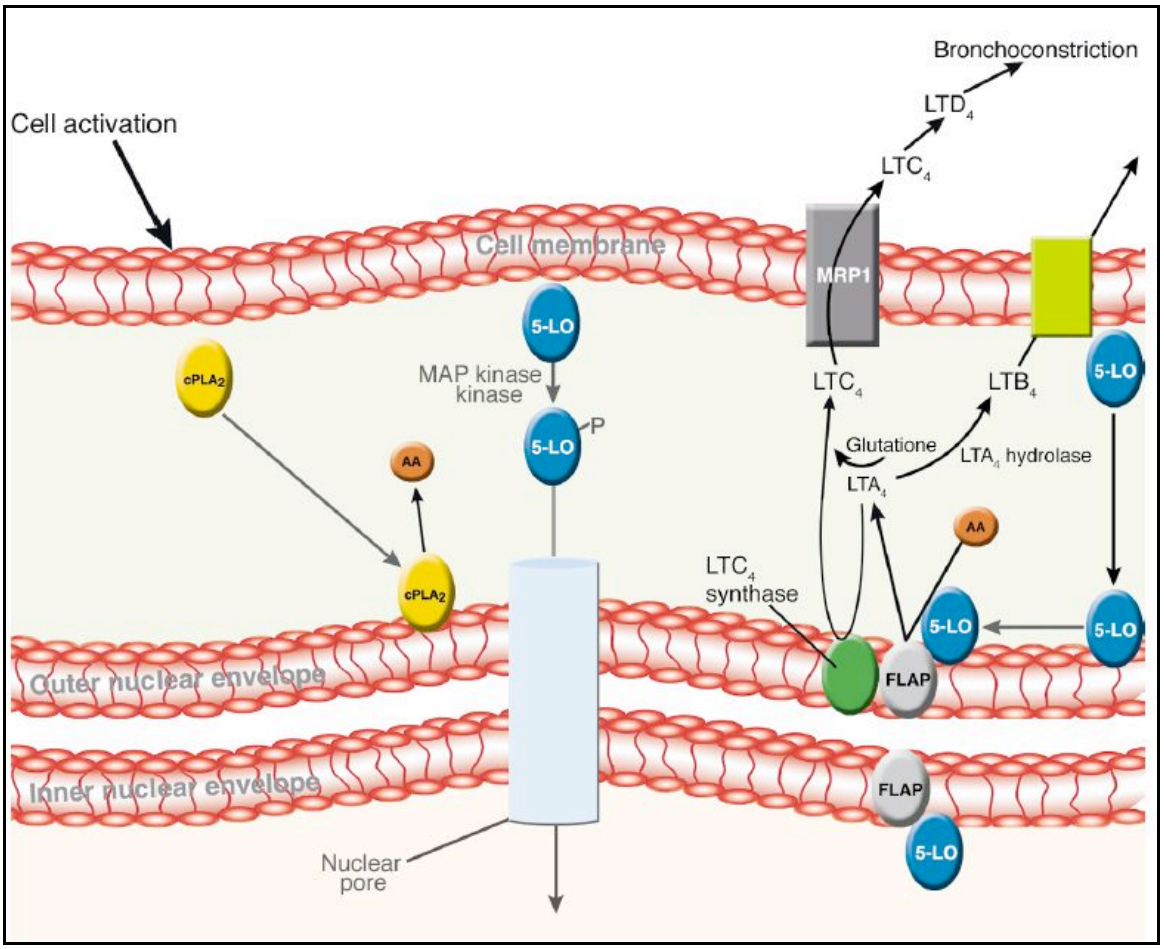

Figure 1.2. The 5-lipoxygenase pathway for leukotriene biosynthesis. This diagram illustrates the multi-step breakdown of arachadonic acid (AA) to form the final products of the 5-lipoxygenase pathway, LTC_4, and its metabolites, LTD_4 and LTE_4 (Soberman and Christmas, 2003)

LTC_4S belongs to the family of Membrane-Associated Proteins in Eicosanoid and Glutathione metabolism (MAPEG) proteins, which include divergent proteins 5-lipoxygenase-activating protein (FLAP), microsomal glutathione *S*-transferase 1, 2, 3 (MGST1, MGST2, MGST3), and prostaglandin E synthase (PTGES) which share 31%, 18%, 44%, 27% and 14% amino acid sequence similarity, respectively (Jakobsson *et al.,* 1999) (Figure 1.3). MK-886, a FLAP inhibitor, which binds a shared and related arachadonic acid binding domain in LTC_4S, also inhibits LTC_4S activity (Vickers *et al*., 1992 and Abramovitz *et al*., 1993). Drugs developed as $CysLT_1$ receptor antagonists

include Pranlukast (Onon®; Ono Pharmaceutical Co, Ltd, Osaka City, Tokyo, Japan), Montelukast Singulair®; Merck & Co, Inc, Whitehouse Station, New Jersey, USA) and Zafirlukast (Accoalte®; AstraZeneca Pharmaceuticals LP, Wilmington, Delaware, USA) and 5-lipoxygeanse inhibitor Zileuton (Zyflo®; Cornerstone Therapeutics Inc, Cary, North Carolina, USA) (Tantisira and Drazen, 2009 and Duroudier *et al*., 2009) but none have yet been established that directly inhibit LTC_4S activity. This is important because LTC_4S represents the only commited enzyme of the 5-lipoxygenase pathway, ensuring the production of the cysteinyl leukotrienes that cause inflammation (Lam, 2003). Although the x-ray crystal structure of LTC_4S has been determined in 2007 by two separate groups (Ago *et al*., 2007 and Molina *et al*., 2007), which is discussed in further details in Chapter 3, we are interested in solving the structure by electron crystallography, which we hope will give us further insight into the native-structure and functionality of this enzyme.

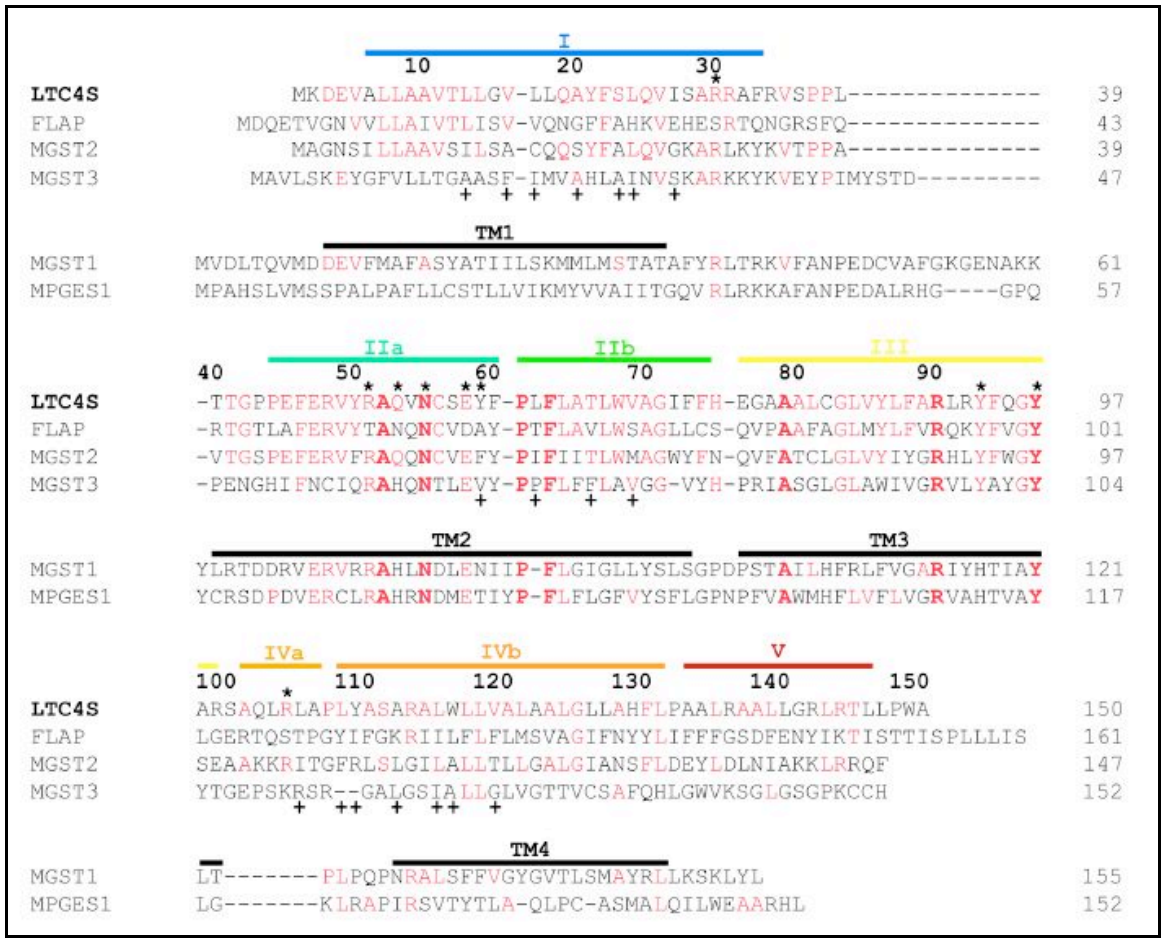

Figure 1.3. Sequence alignment of MAPEG family proteins. Sequence alignment of all proteins within the membrane-associated proteins of eicosanoid and glutathione metabolism (MAPEG) family: leukotriene C4 synthase (LTC_4S), 5-lipoxygenase activating protein (FLAP), microsomal glutathione *S*-transferase 1, 2, & 3 (MGST1, MGST2, & MGST3), and membrane-associated prostaglandin E synthase-1 (mPGES1). Conserved residues are colored red, asterisks (*) denote residues that interact with GSH, and plus (+) signs denote residues that form the LTA_4 binding site which will be discussed in further detail below (Ago *et al.,* 2007).

Arg104s role in substrate activation

An in-depth description of previous works performed of $hLTC_4S$ is summarized in Chapter 3. In 2007 the x-ray crystal structure of substrate-bound LTC_4S was solved by two groups (Ago *et al*., 2007, Molina *et al.*, 2007) revealing important details about glutathione (GSH) binding. In particular, the GSH binding site is located between

adjacent monomers, in a U-shaped cavity close to the cytosolic side of the enzyme. GSH interacts directly with nine residues: Arg51, Tyr97, Arg104, Tyr93, Asn55, Glu58, and Tyr59 from one monomer and Arg30 and Gln53 from a second neighboring monomer (Figure 1.4a and 1.4b). Of these nine amino acid residues, R104 is of particular interest in this study because it was observed to interact with the thiol group of GSH (Ago *et al*., 2007, Molina *et al.,* 2007). It is predicted that R104 abstracts the proton off the thiol group, producing a thiolate anion and activating GSH (GS^-). The activated GS^- can then attach the C6 position of LTA_4, forming a thioether bond. The resulting C5 hydroxyl anion is protonated by R31 of monomer A, forming the final product LTC_4 (Ago *et al*., 2007 and Saino *et al*., 2011). This proposed mechanism can be seen schematically drawn in Figure 1.4c. Another graduate student of the Schmidt-Krey lab, Matthew Johnson, is investigating details of side chain R31, which is implicated in LTA_4 binding.

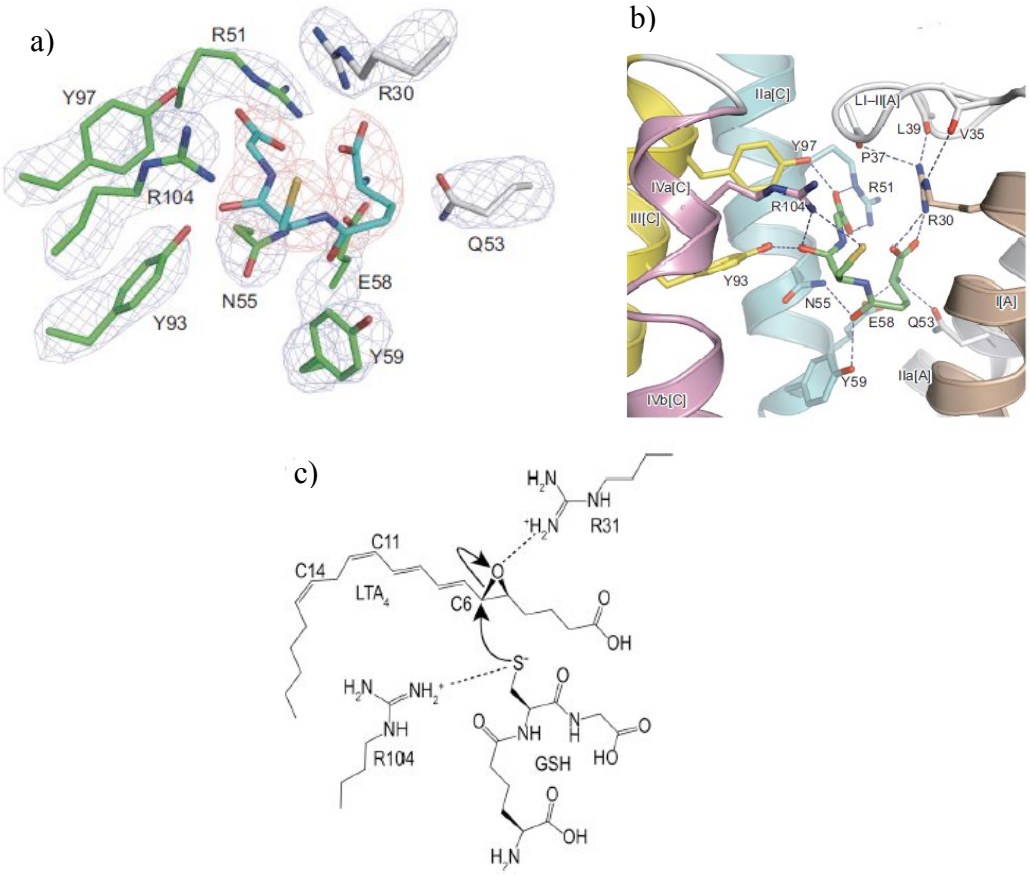

Figure 1.4. Crystal structure of GSH-bound LTC_4S. GSH binding is localized within a cavity between adjacent monomers of LTC_4S. a) Nine amino acid residues interact directly with GSH. Electron density maps of side chains (blue mesh) and GSH (red mesh) are shown, superimposed on stick models of the amino acid side chains of neighboring monomers (Green and silver, respectively). b) electrostatic interactions between GSH and side chains of neighboring monomers, denoted [A] and [C]. Specifically, this includes helices IIa (light blue), III (yellow), and IVa (pink) from monomer C and helices I (brown) and IIa (silver) of monomer A. Arg104 of monomer C, the residue of interest in this study, is shown interacting with the thiol group of GSH (Ago *et al*., 2007). c) Schematic of LTC_4S putative mechanism (Saino *et al*., 2011).

Based on the structural information obtained from the crystal structure of LTC_4S, it is of interest to see what deviations from structure and catalytic mechanism are observed for conjugation of GSH, if we mutate the central amino acid residue implicated

in substrate binding. When R104 was mutated to an alanine (R104A) the enzymes activity was nearly abolished (Saino *et al*., 2011), which lends further support to the importance of this residue in catalytic mechanism. It is of interest to over-express, purify and obtain 2D crystals of mutant R104A, alongside wild-type (WT) LTC_4S, to answer questions related to structure-function changes that may be observed by electron crystallography.

Molecular cloning of $hLTC_4S$ and transformation in *Schizosaccharomyces pombe*

Expression cloning of the cDNA for human leukotriene C4 synthase ($hLTC_4S$) was performed by Lam *et al.* (1994). Transfection of KG-1 cDNA expression library in COS-8 cells was performed, upon which a fluorescence- linked immunoassay for enzymatic product LTC_4 after addition of substrate LTA_4, was used to screen for $hLTC_4S$ activity. Individual clones with maximal $hLTC_4S$ activity contained a 694-bp cDNA insert with an open reading frame encoding a 16.5 kDa protein of 150 amino acids with a pI of 11.05 (Figure 1.5 (Lam *et al.,* 1994). By polymerase chain reaction (PCR), an NdeI restriction site was created at the ATG start codon and His_6-tag created at the C-terminus, of the $hLTC_4S$ cDNA using a sense primer (5'GGTCATATGAAGGACGAGGTAGCT-3') and an antisense primer (5'-CTTGAATTCAGTGATGGTGATGGTGATGGGCC CACGGCAGCAGCGT-3'). The use of C-terminal tags is preferred because it helps ensure that the purified protein is the full-length construct, free of truncation or degradation (Hays, 2010). The fragmented sequence was amplified, subcloned into a pCR-Script vector (Stratagene, La Jolla, CA), and confirmed by DNA sequencing. The NdeI and SmaI fragment was subcloned into a pESP-3 vector (Stratagene) and treated with NdeI and SmaI digestion enzymes to remove the $hLTC_4S$ gene from pESP-3.

Finally, the resultant plasmid was transfected into expression host *Schizosaccharomyces pombe*, genotype h-leu 1-32 (Schmidt-Krey *et al.,* 2004).

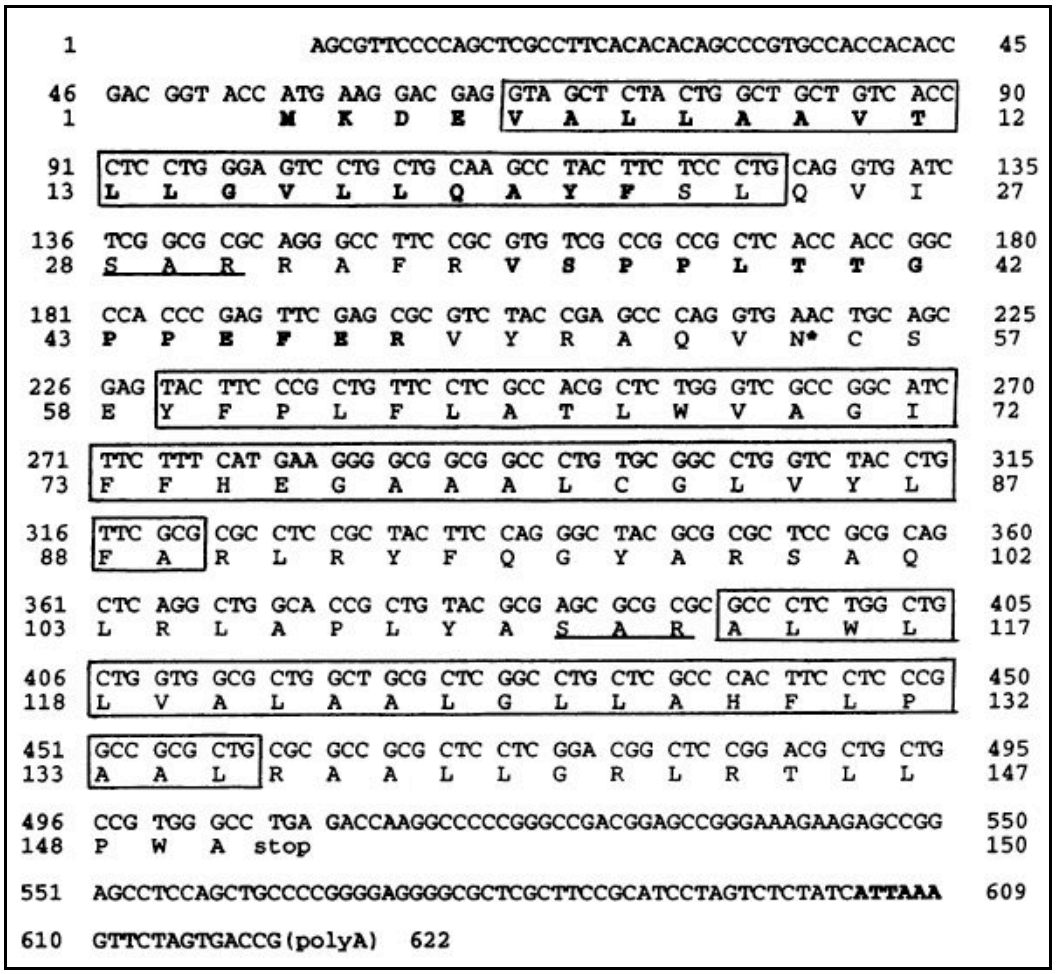

Figure 1.5. hLTC$_4$S DNA and amino acid sequence. Predicted transmembrane helices are boxed, predicted protein kinase C phosphorylation sites are underlined, and potential *N*-linked glycosylation site noted by an asterisk. Numbers represent nucleotide and amino acid positions (Lam *et al.,* 1994)

Induced over-expression of hLTC$_4$S using NMT1 promoter

According to Schmidt-Krey *et al.* (2004) *Schizosaccharomyces pombe* (*S. pombe*) was selected as the host expression system for this study. As mentioned above, over-expression in yeast has many benefits in general (Andre *et al*., 2006 and Wagner *et al*.,

2006), and specifically in *S. pombe* (Yang *et al*., 2009, Chen *et al*., 2011, and Sander *et al*., 1994). The genome of this popular model system was sequenced and annotated in 2002, revealing detailed information about the number of protein-coding genes, centromere length, and identification of conserved genes for eukaryotic cell organization (Wood *et al*., 2002). *S. pombe* is considered to be more closely related to higher eukaryotes than *S. cerevisiae* in several aspects, such as cell cycle regulation and chromosomal organization (Kaufer *et al*., 1985). Several vectors have been developed and are now available for regulated or constitutive expression of heterologous or homologous genes specifically for *S. pombe*, which no longer rely on plasmids derived from *S. cerevisiae* that work at low efficiency in the fission yeast (Siam *et al*., 2004). Thus, the use of *S. pombe* as an expression host for mammalian proteins is more likely to be comparable to its native and biologically functional counterpart (Yang *et al*., 2009).

The nmt1$^+$ (*n*o *m*essage in *t*hiamine) promoter is one of the most frequently used regulatable promoters for *S. pombe* protein expression studies. It was the first promoter to be cloned and characterized in *S. pombe* (Maundrell, 1990). As the name implies, the promoter is tightly repressed in the presence of 0.5 – 15 μM thiamine (vitamin B_1) in the growth media (Yang *et al.,* 2009). Maximum induction is achieved when cells are grown in thiamine-free media for 16 – 20 hours (Forsburg, 2003). It was found that over-expression was achieved when yeast extract + supplements (YES) media was incubated until an optical density measure at 600 nm wavelength, or OD_{600}, of 0.8 – 1.0 was reached (Yang *et al*., 2009). An OD_{600} of 1 equals ~ 1.5 x 10^7 cells per mL, but it should be noted that OD_{600} is a measure of cell mass, not cell number (Forsburg, 2003). YES is the rich medium used for general growth, which contains thiamine for promoter repression; induction necessitates the use of Edinburgh minimal medium (EMM) which is the minimal medium used for regulative induction and mating suppression and contains no thiamine (Forsburg, 2003). *S. pombe* generation time ranges from 2 – 5 hours at

permissive temperatures of 17 – 36°C, with a preferred temperature of 32°C (Siam *et al.,* 2004).

1.2 MATERIALS AND METHODS

Materials

Human LTC_4S ($hLTC_4S$), subcloned into a pESP-3 vector and transfected into *Schizosaccharomyces pombe*, was a generous gift from K. Frank Austen, Harvard Medical School, Massachusetts (Lam *et al*., 1994 and Schmidt-Krey *et al.*, 2004).

Yeast extract + supplement (YES) and Edinburg minimal media (EMM) were both purchased from MP Biomedicals®. Thiamine hydrochloride (vitamin B_1 hydrochloride) was purchased from Sigma-Aldrich®.

Methods

Cell culture and expression

Cell culture and expression was achieved according to Schmidt-Krey *et al*. (2004). Cell culture media was prepared according to the manufacturer. 35 g per L of YES media was prepared and autoclaved at 121°C. Upon cooling to room temperature, filter-sterilized thiamine hydrochloride was added to a final concentration of 5 μM to maintain selection for the plasmid containing $hLTC_4S$. $hLTC_4S$ 50% glycerol stocks, stored at -80°C, were transferred into the YES media. The thiamine-inoculated yeast cell culture was incubated for 18 hours, at 250 rpm and 28°C, until an OD_{600} of 0.8 – 1.0 was obtained. Cells were harvested by centrifugation at 5000 x *g* for 3 minutes at room temperature, until all media was spent and the supernatant discarded. The yeast cell pellet was washed by resuspension with sterile water followed by centrifugation at 5000 x *g* for 3 minutes at room temperature and the supernatant discarded. Expression was induced by resuspending the final yeast pellet in EMM broth (32 g per L in ddH_2O) and

autoclaved at 121°C and cooled to room temperature. The yeast cell culture was finally grown at 30°C at 200 rpm for 16 - 20 hours. After cell culture and expression, the yeast culture was harvested by centrifugation at 5000 x *g* for 3 minutes at room temperature and the supernatant discarded. The final cell pellet was resuspended in 50 % glycerol and stored at -80°C.

1.3 RESULTS AND DISCUSSION

Cell culture conditions control expression levels

The original protocol for cell culture was as follows: inoculate 200 mL YES with individual $hLTC_4S$ *S. pombe* colony. The 200 mL YES was placed into an incubator shaker spinning at 250 rpm and 28°C for a non-specific amount of time, usually 1 – 2 days. After incubation in YES media, the *S. pombe* cells were spun down at 5000 x *g* for 3 minutes until all growth media was spent and supernatant discarded. The YES cell pellet was washed 2 – 3 times in ddH_2O and finally resuspended and transferred to 3 L of fresh EMM media. The 3 L of EMM media was placed into an incubator shaker spinning at 250 rpm and 28°C again, for a non-specific amount of time, anywhere from 2 – 7 days, obtaining on average a 30 g wet cell pellet after cell harvest was complete. At one point, in a further attempt to harvest a larger cell culture population, the EMM was changed out multiple times to supply the cell population with fresh induction media. The rationale behind longer and non-specific incubation times was to obtain a larger population of cells, of which would be expressing our target gene. Upon closer inspection though, it was learned that tighter control of cell harvest conditions yielded higher quantities of target protein. The original cell culture protocol was modified according to Schmidt-Krey *et al.* (2004) and after cell harvest, an average weight of 7g wet cell pellet was obtained per liter of EMM media, after centrifugation at 7000 x *g*. Expression of $hLTC_4S$ is controlled by the $nmt1^+$ promoter. In the presence of thiamine, the promoter is

repressed and gene expression does not occur. Upon removal of thiamine in the growth media, the promoter is turned on and gene expression is also turned on. Figure 1.6 shows sodium dodecyl sulfate-polyacrylamide gel electrophoresis (SDS-PAGE) results after a side-by-side purification of two different cell culturing conditions. The first cell culture was performed with 5 μM thiamine in both YES and EMM media, which should repress any gene expression. The second cell culture was performed with 5 μM thiamine in the YES media only, which should repress gene expression in the YES and allow gene expression in the thiamine-free EMM. All other conditions were held constant, including incubation temperature and time, culture volumes, and overall protein purification methods. After purification using immobilized metal affinity chromatography (IMAC), $hLTC_4S$ was observed, at 18 kDa, only in the elution fractions where thiamine-free EMM media was used during cell culture. This displays the inducible nature of $hLTC_4S$ expression utilizing the $nmt1^+$ promoter.

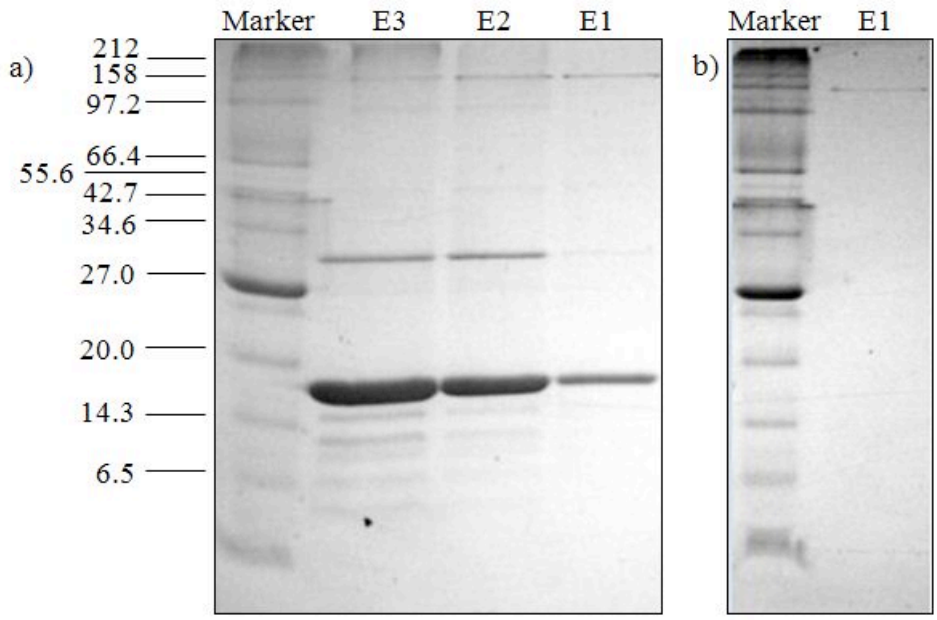

Figure 1.6. SDS-PAGE results comparing cell culture conditions. Cell culture was varied in only one condition: the presence or absence of thiamine. *S. pombe* contains an $nmt1^{+}$ promoter. In the presence of thiamine, gene expression is repressed. In the absence of thiamine, gene expression is permitted. A) Purification results, elution 1 – 3 after IMAC, of cell culture harvest in the absence of thiamine in the EMM culture media. B) Purification results, elution 1 after IMAC, of cell culture harvest in the presence of thiamine in the EMM induction media. $hLTC_4S$ is an 18 kDa MP. Molecular weight, in kDa, denoted to the left.

As mentioned earlier, MP overexpression can become toxic to the cell, which can lead to accumulation within the lumen of the endoplasmic reticulum, triggering the unfolded protein response (UPR) (Griffith *et al.,* 2003). The UPR is a cellular stress response conserved in eukaryotes that aims to restore normal cell function by transiently decreasing protein translation and activating the endoplasmic reticulum-associated protein degradation (ERAD) system (Kaufman *et al.,* 2002). Successful over-expression in eukaryotes requires that translation of functional protein in the ER not exceed threshold levels that induce the UPR (Griffith *et al*., 2003). Also mentioned earlier is the presence of endogenous proteases found in vacuoles of yeast that can affect protein integrity (Jones, 2002). This could explain why longer cell culture times produced no

visible gene expression, because protein degradation occurred after maximal expression was achieved. A possible alternative is the use of a previously published truncated derivative of the $nmt1^+$ promoter (Kumar and Singh, 2006), which was found to repress expression in the presence of thiamine, but displayed temperature-dependent expression in the absence of thiamine: repression at 36°C and induction at 25°C, whereas full-length $nmt1^+$ expresses at both temperatures. $Nmt1^+$ allows expression and maximum protein levels in 15 – 18 hours, whereas this truncated promoter construct can achieve maximal expression in only 3 hours. This is advantageous because cells are exposed to possibly toxic levels of expressed protein for shorter induction times and because proteolysis levels may be reduced (Kumar and Singh, 2006).

1.4 CONCLUSIONS

The over-expression of $hLTC_4S$ was successfully achieved using previously established methods. Expression was induced by growth in thiamine-free media, which turns on the $nmt1^+$ promoter and allows gene expression to occur. MP over-expression can become toxic to the cell and may lead to issues such as degradation by endogenous proteases or accumulation in the endoplasmic reticulum by activation of the unfolded protein response (UPR). Instead, tight control of cell harvest conditions via the $nmt1^+$ promoter by monitoring OD_{600}, removing thiamine from the induction EMM media, and culturing times between 16 – 20 hours proved to be the most useful determinants in the over-expression of $hLTC_4S$.

1.5 APPENDIX

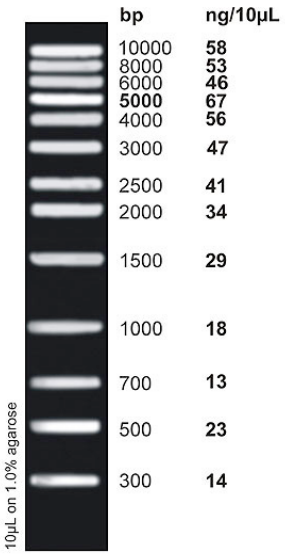

FIGURE A.1. Fisher BioReagents® exACTGene® DNA Ladders > 1kb DNA Ladder.

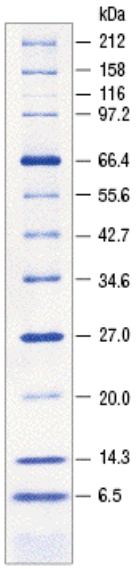

Figure A.2. New England BioLabs® Inc., Protein Marker, Broad Range (2 – 212 kDa).

1.6 BIBLIOGRAPHY

Abeyrathne, P.D., Chami, M., Pantelic, R.S., Goldie, K.N., Stahlberg, H., 2010. Preparation of 2D crystals of Membrane Proteins for High-Resolution Electron Crystallography Data Collection. *Methods in Enzymology* 481 (10), 81001 - 81008.

Abramovitz, M., Wong, E., Cox, M.E., Richardson, C.D., Li, C., Vickers, P.J., 1993. 5-lipoxygenase-activating protein stimulates the utilization of arachadonic acid by 5-lipoxygenase. *European Journal of Biochemistry* 215 (1), 105 - 111.

Ago, H., Kanaoka, Y., Irikura, D., Lam, B.K., Shimamura, T., Austen, K.F., Miyano, M., 2007. Crystal structure of a human membrane protein involved in cysteinyl leukotriene biosynthesis. *Nature* 448 (7153), 609 - 612.

Andre, N., Cherouati, N., Prual, C., Steddan, T., Zeder-Lutz, G., Magnin, T., Pattus, F., Michel, H., Wagner, R., Reinhart, C., 2006. Enhancing functional production of G-protein coupled receptors in Pichia pastoris to levels required for structural studies via a single expression screen. *Protein Science* 15 (5), 1115 - 1126.

Appel, M., Hizlan, D., Vinothkumar, K.R., Ziegler, C., Kühlbrandt, W., 2009. Conformations of NhaA, the Na/H exchanger from Escherichia coli, in the pH-activated and ion-translocating states. *Journal of Molecular Biology* 386 (2), 351 - 365.

Auer, M., Kim, M.J., Lemieux, M.J., Villa, A., Song, J., Li, X., Wang, D., 2001. High-yield expression and functional analysis of Escherichia coli glycerol-3-phosphate transporter. *Biochemistry* 40 (22), 6628 - 6635.

Bharathi, A., Ghosh, A., Whalen, W.A., Yoon, J.H., Pu, R., Dasso, M., Dhar, R., 1997. The human RAE1 gene is a functional homologue of Schizosaccharomyces pombe rae1 gene involved in nuclear export of Poly(A)+ RNA. *Gene* 198 (1-2), 251 - 258.

Binda, C., Li, M., Hubalek, F., Restelli, N., Edmondson, D.E., Mattevi, A., 2003. Insights into the mode of inhibition oh human mitochondrial monoamine oxidase B from high-resolution crystal structures. *Proc Natl Acad Sci.* 100 (17), 9750 - 9755.

Bogdanov, M., Umeda, M., Dowhan, W., 1999. Phospholipid0assisted refolding of an integral membrane protein. *Journal of Biological Chemistry* 274 (18), 12339 – 12345.

Christmas, P., Weber, B.M., McKee, M., Brown, D., Soberman, R.J., 2002. Membrane localization and topology of leukotriene c4 synthase. *Journal of Biological Chemistry* 277 (32), 28902 – 28908.

Cohen, S.L., and Chait, B.T., 2001, Mass spectrometry as a tool for protein crystallography. *Annual Review of Biophysics and Biomolecular Structure* 30, 67 – 85.

Cooper, M.A., 2004. Advances in membrane receptor screening and analysis. *Journal of Molecular Recognition* 17 (4), 286 – 315.

Daley, D.O., Rapp, M., Granseth, E., Melen, K., Drew, D. von Heijne, G., 2005. Global topology analysis of the Escherichia coli inner membrane proteome. *Science* 308 (5726), 1321 – 1323.

Drew, D., Froderberg, L., Baars, L., de Gier, J.L., 2003. Assembly and overexpression of membrane protein in Escherichia coli. *Biochimica et Biophysica Acta* 1610 (1), 3 – 10.

Drews, J., 2000. Drug discover: a historical perspective. *Science* 278 (5460), 1960 – 1964.

Duroudier, N.P., Tulah, A.S., Sayers, I., 2009. Leukotriene pathway genetics and pharmacogenetics in allergy. *Allergy* 64 (6), 823 – 839.

Fischer, G., Kosinska-Erisson, U., Aponte-Santamaria, C., Palmgren, M., Geijer, C., Hedfalk, K., Hohmann, S., de Groot, B.L., Neutze, R., Lindkvist-Petersson, K., 2009. Crystal structure of a yeast aquaporin at 1.15 angstrom reveals a novel gating mechanism. *PLoS Biology* (7) 6, e10000130.

Forsburg, S.L., 2003. S. pombe strain maintenance and media. *Current Protocols in Molecular Biology* 13.15, 1 – 5.

Glover, S., *et al.,* 1995. Translocation of the 85-kDa phospholipase A2 from cytosol to the nuclear envelope in rat basophilic leukemia cells stimulated with calcium ionophore or IgE/antigen . *Journal of Biological Chemistry* 270, 2256 – 2261.

Griffith, D.A., Delipala, C., Leadsham, J., Jarvis, S.M., Oesterhelt, D., 2003. A novel yeast expression system for the overproduction of quality-controlled membrane proteins. *FEBS Letters* 553 (1 – 2), 45 – 50.

Grishammer, R., and Tate, C.G., 1995. Overexpression of integral membrane proteins for structural studies. *Quarterly Review of Biophysics* 28 (3), 315 – 422.

Hui, Y. *et al.,* 2001. The murine cysteinyl leukotriene 2 (CysLT2) receptor. cDNA and genomic cloning, alternative splicing, and in vitro characterization. *Journal of Biological Chemistry* 276, 47489 – 47495.

Jakobsson, P.J., Morgenstern, R., Mancini, J., Ford-Hutchinson, A., Persson, B., 1999. Common structural features of MAPEG- A widespread superfamily of membrane associated proteins with highly divergent functions in eicosanoid and glutathione metabolism. *Protein Science* 8, 689 – 692.

Jedlitschky, G., Buchholz, U., Keppler, D., 1994. Characterization of the ATP-dependent leukotriene C4 export carrier in matocytoma cells. *J. Biochem.* 220, 599 – 563.

Jones, E.W., 2002. Vacuolar proteases and proteolytic artifacts in saccharomyces cerevisiae. *Methods in Enzymology* 351, 127 – 150.

Kargman, S., Vickers, P.J., Evans, J.F., 1992. A23187-induced translocation of 50lipoxygenase in osteosarcoma cells. *Journal of Cell Biology* 119, 1701 – 1709.

Kaufer, N.F., Simanis, V., Nurse, P., 1985. Fission yeast Schizosaccharomyces pombe correctly excises a mammalian RNA transcript intervening sequence. *Nature* 318 (6041), 78 – 80.

Kaufman, R.J., Scheuner, D., Schroder, M., Shen, C., Lee, K., Liu, C.Y., Arnold, S.M., 2002. The unfolded protein response in nutrient sensing and differentiation. *Nature Reviews: Molecular Cell Biology* 3 (6), 411 – 421.

Kozak, M., 1991. Structural features in eukaryotic mRNAs that modulate the initiation of translation. *The Journal of Biological Chemistry* 30 (25) 19867 – 19870.

Kozak, M., 1992. Regulation of translation in eukaryotic systems. *Annual Review of Cell Biology* 8, 197 – 225.

Kühlbrandt, W., 2012. Combining cryo-EM and x-ray crystallography to study membrane protein structure and function. Macromolecular Crystallography: Deciphering the Structure, Function and Dynamics of Biological Molecules. Ed. Maria Armenia Carronda and Ed. Paola Spadon. 1st. Dodrecht: Springer, 2012, 93 – 101.

Kumar, R. and Singh, J., 2006. A truncated derivative of nmt1 promoter exhibits temperature-dependent induction of gene expression in Schizosaccharomyces pombe. *Yeast* 23 (1), 55 – 65.

Krebs, A., Edwards, P.C., Villa, C., Li, K., Schertler, G.F., 2003. The three-dimensional structure of bovine rhodopsin determined by electron cryomicroscopy. *Journal of Biological Chemistry* 278 (50), 50217 – 50225.

Lam, B.K., Owen, W.F., Austen, K.F., Soberman R.J., 1989. The identification of a distinct export step following the biosynthesis of leukotriene C4 by human eosinophils. *Journal of Biological Chemistry* 264, 12885 – 12889.

Lam, B.K., Penrose, J.F., Freeman, G.J., Austen, K.F., 1994. Expression cloning of a cDNA for human leukotriene c4 synthase, an integral membrane protein conjugating reduced glutathione to leukotriene a4. *Biochemistry* 91 (16), 7663 – 7667.

Lam, B.K., 2003. Leukotriene c4 synthase. *Prostaglandins, Leukotrienes and Essential Fatty Acids* 69 (2 -3), 111 – 116.

Lappano, R. and Maggiolini, M., 2011. G protein-coupled receptors: novel targets for drug discovery in cancer. *Nature Reviews Drug Discovery* 10, 47 – 60.

Lewis, R.A., Austen, K.F., Soberman, R.J., 1990. Leukotrienes and other products of the 5-lipoxygenase pathway. Biochemistry and relation to pathobiology in human diseases. *New England Journal of Medicine* 323, 645 – 655.

Loe, D.W., Almquist, K.C., Deeley, R.G., and Cole, S.P.C., 1996. Multidrug resistance protein (MRP)-mediated transport of leukotriene C4 and chemotherapeutic agents in membrane vesicles. *J. Biol. Chem.* 271, 9675 – 9683.

Lynch, K.R., *et al.,* 1999. Characterization of the human cysteinyl leukotriene CysLT1 receptor. *Nature* 399, 78 – 93.

Maundrell, K., 1990. Nmt1 of fission yeast: a highly transcribed gene completely repressed by thiamine. *Journal of Biological Chemistry* 265 (19), 10857 – 10864.

Miroux, B., and Walker, J.E., 1996. Over-production of proteins in Escherichia coli: mutant hosts that allow synthesis of some membrane proteins and globular proteins at high levels. *Journal of Molecular Biology* 260 (3), 289 – 298.

Molina, D.M., Wetterholm, A., Kohl, A., McCarthy, A.A., Niegowski, D., Ohlson, E., Hammarberg, T., Eshaghi, S., Haeggerstrom, J.Z., Nordlund, P., 2007. Structural basis for synthesis of inflammatory mediators by human leukotriene c4 synthase. *Nature* 448 (7153), 613 – 617.

Morosinotto, T., Bassi, R., Frigerio, S., Finazzi, G., Morris, E., Barber, J., 2006. Biochemical and structural analyses of a higher plant photosystem II supercomplex of a photosystem I-less mutant of barley. Consequences of a chronic over-reduction of the plastoquinone pool. *The FEBS journal* 273 (20), 4616 – 4630.

Nicholson, D.W., Ali, A., Vaillancourt, J.P., Calaycay, J.R., Mumford, R.A., Zamboni, R.J., Ford-Hutchinson, A.W., 1993. Purification to homogeneity and the N-terminal sequence of human leukotriene c4 synthase: a homodimeric glutathione S-transferase composed of 18-kDa subunits. *Proc. Natl. Acad. Sci.* 90, 2015 – 2019.

Oesterhelt, D. and Stoeckenius, W., 1974. Isolation of the cell membrane of Halobacterium halobium and its fractionation into red and purple membrane. *In Methods Enzymol.* 31, 667 – 678.

Parcej, D.N. and Eckhardt-Strelaur, L., 2003. Structural characterization of neuronal voltage-sensitive K^+ channels heterologously expressed in Pichia pastoris. *Journal of Molecular Biology* 333 (1), 103 – 116.

Penrose, J.F., Spector, J., Baldasaro, M., Xu, K., Boyce, J., Arm, J.P., Austen, K.F., Lam, B.K., 1996. Molecular cloning of the gene for human leukotriene c4 synthase. *Journal of Biological Chemistry* 271 (19), 11356 – 11361.

Radmark, O., Shimizu, T., Jornvall, H., and Samuelsson, B., 1988. Leukotriene a4 hydrolase in human leukocytes. Purification and properties. *Journal of Biological Chemistry* 259, 12339 – 12345.

Renault, L., Chou, H., Chiu, P., Hill, R.M., Zeng, X., Gipson, B., Zhang, Z.Y., Cheng, A., Unger, V., Stahlberg, H., 2006. Milestones in electron crystallography. *Journal Computationally Aided Molecular Design* 20 (7 – 8), 519 – 527.

Rouzer, C.A., Matsumoto, T., and Samuelsson, B., 1986. Single protein from human leukocytes possesses 5-lipoxygenase and leukotriene a4 synthase activities. *Proc. Natl. Acad. Sci. U.S.A.* 83, 857 – 861.

Rouzer, C.A. and Kargman, S., 1988. Translocation of 5-lipoxygenase to the membrane in human leukocytes challenged with ionophore A23187. *Journal of Biological Chemistry* 263, 10980- 10988.

Saino, H., Ukita, Y., Ago, H., Irikura, D., Nisawa, A., Ueno, G., Yamamoto, M., Kanaoka, Y., Lam, B.K., Austen, K.F., Mirano, M., 2011. The catalytic architechture of leukotriene c4 synthase with two arginine residues. *Journal of Biological Chemistry* 286 (18), 16392 – 16401.

Samuelsson, B., *et al.,* 1987. Leukotrienes and lipoxins: structures, biosynthesis, and biological effects. *Science* 237, 1171 – 1177.

Sander, P., Grunewald, S., Reilander, H., Michel, H., 1994. Expression of the human D2S dopamine receptor in the yeasts Saccharomyces cerevisiae and Schizosaccharomyces pombe: a comparative study. *FEBS Letters* 344 (1), 41 – 46.

Schmidt-Krey, I., Kanaoka, Y., Mills, D.J., Irikura, D., Haase, W., Lam, B.K., Austen, K.F., Kühlbrandt, W., 2004. Human leukotriene c4 synthase at 4.5 angstrom resolution in projection. *Structure* 12 (11), 2009 – 2014.

Shouffani, A. and Kanner, B.I., 1990. Cholesterol is required for the reconstitution of the sodium- and chloride- coupled, gamma-aminobutyric acid transporter from rat brain. *Journal of Biological Chemistry* 265 (11), 6002 – 6008.

Siam, R., Dolan, W.P., Forsburg, S.L., 2004. Choosing and using Schizosaccharomyces pombe plasmids. *Methods* 33 (3), 189 – 198.

Soberman, R.J. and Christmas, P., 2003. The organization and consequences of eicosanoid signaling. *Journal of Clinical Investigation* 111 (8), 1107 – 1113.

Strid, T., Svartz, J., Franck, N., Hallin, E., Ingelsson, B., Soderstrom, M., Hammarstrom, S., 2009. Distinct parts of leukotriene c4 synthase interact with 5-lipoxygenase and 5-lipoxygenase activating protein. *Biochemical and Biophysical Research Communications* 381 (4), 518 – 522.

Tantisira, K.G. and Drazen, J.M., 2009. Genetics and pharmacogenetics of the leukotriene pathway. *Journal of Allergy and Clinical Immunology* 124 (3), 422 – 427.

Tate, C.G., 2001. Overexpression of mammalian integral membrane proteins for structural studies. *FEBS Letters* 504 (3), 94 – 98.

Taylor, G.W., *et al.,* 1989. Urinary LTE4 after antigen challenge in acute asthma and allergic rhinitis. *Lancet* 1, 584 – 588.

Vickers, P.J., Adam, M., Charleson, S., Coppolino, M.G., Evans, J.F., Mancini, J.A., 1992. Identification of amino acid residues of 5-lipoxygenase activating protein essential for the binding of leukotriene biosynthesis inhibitors. *Molecular Pharmacology* 42 (1), 94 – 102.

Wagner, S., Bader, M., Drew, D., de Gier, J., 2006. Rationalizing membrane protein overexpression. *TRENDS in Biotechnology* 24 (8), 364 - 371.

Wagner, S., Baars, L., Ytterberg, A.J., Klussmeier, A., Wagner, C.S., Nord, O., Nygren, P.A., van Wijk, K.J., de Gier, J.W., 2007. Consequences of membrane protein overexpression in Escherichia coli. *Molecular Cell Proteomics* 6 (9), 1527 – 1550.

White, M.A., Clark K.M., Grayhack, E.J., Dumont, M.E., 2007. Characteristics affecting expression and solubilization of yeast membrane proteins. *Journal of Molecular Biology* 365 (3), 621 – 636.

Wood, V., Gwilliam, R., Rajandream, M.A., Lyne, M., *et al*., 2002. The genome sequence of Schizosaccharomyces pombe. *Nature* 415 (6874), 871 – 880.

Yang, Y., Hu, Z., Liu, Z., Wang, Y., Chen, X., Chen, G., 2009. High human GLUT1, GLUT2, and GLUT3 expression in Schizosaccharomyces pombe. *Biochemistry (Moscow)* 74 (1), 75 – 80.

Yoshimoto, T., Soberman, R.J., Spur, B., Austen K.F., 1988. Properties of highly purified leukotriene c4 synthase of guinea pig lung. *Journal Clinical Investigation* 81, 866–871.

CHAPTER 2

2. PURIFICATION OF HUMAN LEUKOTRIENE C4 SYNTHASE

2.1 BACKGROUND AND SIGNIFICANCE

Membrane protein purification overview

The purification of MPs vary from that of soluble proteins in that MPs require the use of detergents to help remove the protein from the lipid bilayer in a process called solubilization. Detergents are amphipathic molecules that mimic characteristic traits of lipid molecules within the membrane (Seddon *et al.,* 2004). Ideally, the detergent(s) used to solubilize the MP should efficiently remove the protein from its native host membrane, a heterogeneous and dynamic mosaic lipid bilayer, while maintaining the enzymes structure and functional activity (Abeyrathne *et al.,* 2010). Overall, MP purification can be organized into two major steps: isolating membranes and purifying the target protein, which is described in detail below.

Isolating membranes

The lipid bilayer is a complex environment composed of several different types of lipid molecules; in order to reduce such complexities it is necessary to transfer the target protein to a more homogenous environment, such as a detergent micelle, and to remove other contaminant proteins. In order for this to be done, the cell must first be disrupted to expose and free cellular components including membranes that contain the target protein. After cell lysis, the target protein is removed from the lipid membrane of the expression host by solubilizing the MP in detergent. MPs are not soluble in aqueous solutions, and thus the goal is to obtain a water-soluble complex of protein-detergent molecules (Newby *et al.,* 2009). They are extracted form their native membrane by detergents, ampiphilic molecules with a polar head group and a hydrophobic chain, that satisfy the MPs need to

be surrounded by a hydrophobic environment at transmembrane segments, and introducing cytosolic loops and domains to an aqueous phase (Seddon *et al*., 2004). The detergent of choice is important because it determines MP solubility and stability and can affect the type and amount of co-purified lipids that remain after solubilization, purification, and crystallization (Aveldano, 1996 and Banerjee *et al*., 1995). Co-purified lipids sometimes help to maintain protein stability and/or are essential to enzyme activity, and so excessive solubilization should not be pursued as it may deactivate the enzyme (Mosser, 2001).

There are four classes of detergents: ionic, non-ionic, bile acid salts, and zwitterionic (Figure 2.1). Ionic detergents, such as sodium dodecyl sulfate (SDS), have a charged head group with a hydrocarbon or steroidal backbone. Ionic detergents (Figure 2.1a) are efficient solubilizers, but also denaturing. Bile acid salts (Figure 2.1b) are ionic detergents that have rigid steroidal backbones resulting in a polar and apolar face, and no defined head group. Bile acid salts are mild detergents and less denaturing than ionic detergents. Non-ionic detergents (Figure 2.1c) have characteristic uncharged hydrophilic head groups. These detergents are mild, relatively non-denaturing, and do not affect protein structure. Non-ionic detergents break lipid-lipid and lipid-protein interactions and do not interfere with protein-protein interactions. Finally, zwitterionic detergents (Figure 2.1d) have features similar to ionic and non-ionic detergents. In general, they are denaturing detergents (Seddon *et al.,* 2004).

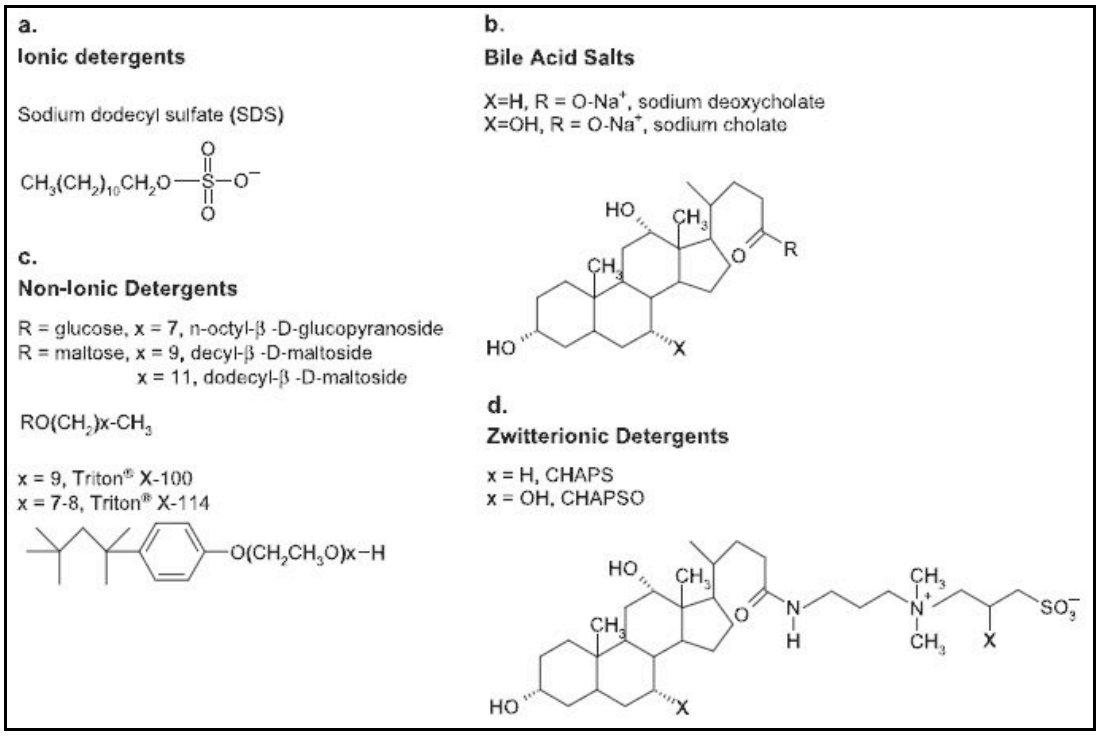

Figure 2.1. Detergent classification. The four classes of detergents, ionic, bile acid salts, nonionic, and zwitterionic detergents, are listed here, with respective molecular formulas (Seddon *et al.,* 2004).

For the solubilization and purification of $hLTC_4S$, two detergents are utilized: bile acid salt sodium deoxycholic acid (Na-DOC) and non-ionic detergent Triton X-100 (TX-100). Detailed properties of both detergents are listed in Table 2.1.

Table 2.1. Properties of detergents used in the solubilization and purification of $hLTC_4S$. The table summarizes properties of sodium deoxycholic acid (Na-DOC) and Triton X-100 (TX-100).

Detergent	Classification	Monomer, MW	Micelle, MW	CMC % (w/v)	CMC Molarity	Aggregation number
Sodium deoxycholate (Na-DOC)	Bile acid salt	414.6 g	2,000 g	0.08 – 0.25%	2 – 6 mM	5
Triton X-100 (TX-100)	Non-ionic	647 g	90,000g	0.015 %	0.24 mM	140

The cellular membranes are solubilized by detergent(s) at a concentration about 10X above the critical micelle concentration (CMC), for 12 – 14 hours at 4°C (Hays *et al*., 2010). At concentrations equal to or above the CMC detergent monomers begin to self-associate and form micelles. At concentrations well above the CMC, these detergent micelles can extract MPs from their native lipid membranes, producing a mixed micelle population of protein-detergent-lipid complexes, detergent-only micelles, and detergent monomers (Figure 2.2). Unsolubilized material can then be removed by high-speed ultracentracentrifugation at > 100,000 x *g*, where they will be found in the pellet. This helps to concentrate the MPs and remove soluble proteins that can degrade the target protein (Newby *et al.,* 2009). The MP of interest has now been removed from its native cellular membrane and is in a soluble form. By definition, a solubilized protein is that of a MP surrounded by a detergent micelle and co-purified lipid molecules from the expression host (Hays *et al*., 2010).

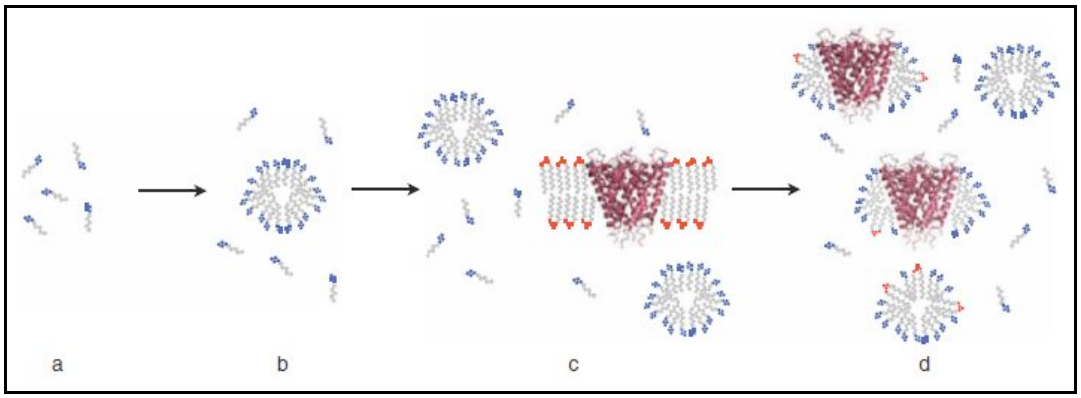

Figure 2.2. Detergent solubilization of MPs. At or above the critical micelle concentration (CMC), detergent monomers (blue) will begin to self-associate and form micelles (a, b). Detergent micelles can then extract MPs from their native lipid bilayers (red) (c), forming a combination of protein-detergent-lipid complexes, detergent-only micelles, and detergent monomers (Newby *et al.,* 2009).

One final consideration during MP solubilization is the critical micellar temperature (cmt), also known as the Kraft Point. The cmt represents the temperature at which detergent monomers, detergent micelles and solid, crystalline detergent are in equilibrium. Only above the cmt will detergent monomers dissolve to form micelles and be able to solubilize MPs (Seddon *et al*., 2004). This is problematic because solubilization and purification steps for $hLTC_4S$ are conducted at 4°C, which may be lower than the cmt for Tx-100 and Na-DOC. One study found that detergent micellar formation decreased with falling temperatures (Aveldano, 1995), most likely due to the inverse relationship between CMC and temperature: as temperature rises, CMC values decrease (Helenius *et al*., 1975). The cmt value is experimentally unknown for most detergents.

Purifying protein

After detergent solubilization of the cellular membranes, it is necessary to isolate and purify $hLTC_4S$ from the remaining soluble proteins in order to obtain a pure,

homogenous and stable sample (Hays *et al*., 2010). Throughout the purification it is necessary to keep the concentration of detergents in all buffers above their respective CMCs to prevent the protein from precipitating and crashing out of solution (Abeyrathne *et al*., 2010). A variety of chromatographic techniques are available to assist in the purification of MPs, such as immobilized metal affinity (IMAC), size-exclusion (SEC), and ion-exchange chromatography (Hays *et al*., 2010). IMAC and buffer exchange were employed to purify C-terminal His_6-tagged $hLTC_4S$. IMAC is a type of affinity chromatography that utilizes histidine residues on the surface of proteins or recombinant proteins with engineered histidine tags. It is composed of metal ligands (Ni^{2+}, Co^{2+}, Zn^{2+}, Cu^{2+}) covalently bound to a stationary phase, soft-gel nitrilotriacetic (NTA) matrix agarose (Porath, 1992). These metal ions coordinate and bind specifically to histidine residues, where coordination occurs between an immobilized metal ion and electron donors from the protein surface (Porath, 1992). After Ni-NTA binding, the agarose is washed with small concentrations (30 mM) imidazole, which helps to remove non-specific, low-affinity bound proteins and reduce the presence of background contaminant proteins, without interfering with His_6-tagged protein binding. Finally, the Ni-NTA bound protein is eluted off the column with high concentrations of imidazole (100 – 250 mM), which displaces the His_6-tagged protein from the Ni-NTA agarose. After IMAC, eluted fractions contain ~90% pure protein. Other advantages of IMAC include ligand stability, high protein loading (5 – 50 mg His-tagged protein per 1 mL of Ni-NTA agarose resin), mild elution conditions, easy regeneration and low cost (Gaberc-Porekar and Menart, 2001). Use of a His-tag also has its own advantages: modest size, smaller than most other purification tags; uncharged at physiological pH, and it has been shown to not interfere with protein structure and function (Gaberc-Porekar and Menart, 2001 & 5Prime PerfectPro® Ni-NTA System Manual).

2.2 MATERIAL AND METHODS

Materials

4-(2-hydroxyethyl)-1-piperazineethanesulfonic acid (HEPES) was purchased from Angus™ Chemicals, sodium chloride (NaCl) from BDH®, glycerol biotechnology grade from Amresco®, 2-mercaptoethanol from OmniPur®, imidazole from Acros®, ethylenediaminetetraacetic acid (EDTA) from Fischer Bioreagents®, L-glutathione reduced 97% (GSH) from Alfa Aesar®, and potassium chloride reagent ACS (KCl) from Acros®.

Detergents for solubilization, Triton X-100 and Na-DOC, were purchased from MP Biomedicals® and Fisher Scientific®, respectively.

Ni^{2+} charged resin for IMAC purification of histidine-tagged $hLTC_4S$ was purchased from 5Prime®.

Glycine was purchased from Sigma® Life Sciences, Coomassie® Brilliant Blue R-250 from Amresco®, bromophenol sodium salt from OmniPur®, protein marker (broad range 2 – 212 kDa from New England BioLabs® Inc., ammonium persulfate (APS) from MP Biomedicals®, N,N'-methylenebisacrylamine (bisacrylamide) from USB® Corporation, tris(hydroxymethyl)aminomethane (Tris) from Fisher Scientific®, and N, N, N, N'-tetramethylethylenediamine (TEMED) from GE Healthcare®, and Tween-20 from BDH® Chemicals.

Methods

Membrane isolation

$hLTC_4S$ was purified according to Schmidt-Krey *et al.* (2004). Cells over-expressing $hLTC_4S$ were broken by mechanical lysis using the BioSpec® BeadBeater in ice cold Break Buffer (50 mM HEPES, pH 7.6; 10% glycerol, 0.5 M NaCl). Successful cell lysis was confirmed visually using a light microscope. After lysis, the cell-free lysate

was centrifuged at 7000 x *g* for 15 minutes at 4°C. Unbroken cells, nuclei, and mitochondria remain in the pellet; soluble protein microsomes and other organelles remain in the supernatant. The pellet was discarded and the supernatant retained. The supernatant was then spun down at 200,000 x *g* for 2 hours at 4°C to collect the membranes. Soluble proteins remain in the supernatant and the microsomes and other organelles are found in the pellet. Above the dark brown hard pellet, a brown-beige layer of loose, liquid soft pellet is observed, where expressed protein is found. Both hard and soft pellets were carefully collected for detergent solubilization.

Detergent solubilization

Membranes obtained from the previous step were solubilized in 1% (v/v) TX-100 and 0.5% (w/v) Na-DOC on ice for 2 – 3 hours, with gentle nutation. After detergent solubilization, any remaining unsolubilized material was removed by centrifugation at 18,000 x *g* for 30 minutes at 4°C.

Ni-NTA protein purification

Immobilized metal affinity chromatography (IMAC) was performed to purify the C-terminal His_6-tagged $hLTC_4S$ from the detergent solubilized lysate. Detergent-solubilized $hLTC_4S$ was mixed with 2 mL of PerfectPro Ni-NTA agarose. After 2 hours of Ni-NTA agarose binding, the lysate was transferred to a gravity column for column purification. Incubation times greater than 3 hours are not recommended as it does not improve $hLTC_4S$ binding and may instead increase potential proteolysis and contaminant binding (Hays *et al*., 2010). Next, very carefully, so as not to disturb the Ni-NTA agarose bed, the protein-bound agarose was washed with 50 CVs of wash I (50 mM HEPES, pH 7.6, 10% glycerol, 0.5 M NaCl, 45 mM imidazole, 1% TX-100, 0.5% Na-DOC) and 25 CVs of wash II (50 mM HEPES, pH 7.6, 10% glycerol, 0.5 M NaCl, 70

mM imidazole, 1% TX-100, 0.5% Na-DOC). The protein was eluted off the column with 5 CVs of elution buffer (50 mM HEPES, pH 7.6, 10% glycerol, 0.5 M NaCl, 300 mM imidazole, 1% TX-100, 0.5% Na-DOC, 1 mM GSH, 1 mM EDTA, 10 mM 2-mercaptoethanol, and 50 mM KCl). When pouring the elution buffer into the gravity column, it is important not to disturb the Ni-NTA agarose bed and to reduce the flow rate during elution, as this will ensure that fractions collected from the column will be well-resolved to the first 3 – 4 fractions and/or mLs.

Buffer exchange

After IMAC purification of $hLTC_4S$, the eluted protein fractions are then processed further by buffer exchange using the ÄKTAprime plus chromatography system and the 5 mL HiTrap Desalting Column. The elution fractions collected from the IMAC column and the desalting buffer (50 mM HEPES, pH 7.6, 0.1 M NaCl, 10% glycerol, 1% TX-100, 0.5% Na-DOC, 1 mM GSH, 1 mM EDTA, 10 mM 2-mercaptoethanol, and 50 mM KCl) were filter sterilized (0.1 μm pore size) to remove any aggregated material. After running a System Wash Method, the Manual Run method and the PrimeView software was used to monitor ultraviolet (UV) light and conductivity readings. Once the UV reading began to rise, the sample was eluted off the column. Protein elutions were collected between UV peaks, before conductivity began to rise. This was performed for all IMAC protein fractions. The detergent solubilized and purified protein was stored at -80°C prior to two-dimensional crystallization trials.

Protein detection: Western blot and SDS-PAGE

Detecting the presence of the purified protein $hLTC_4S$ was achieved by sodium dodecyl sulfate polyacrylamide gel electrophoresis (SDS-PAGE). Samples collected through the course of the purification were treated with 5X SDS loading buffer (250 mM

Tris-HCl, pH 6.8; 10% SDS, 305 glycerol, 5% 2-mercaptoethanol, 0.02% bromophenol blue) and run on a 16% SDS-PAGE gel. After electrophoresis the gels were stained with staining solution (0.3% Coomassie Brilliant Blue R-250, 50% methanol, 10% acetic acid, and 40% ddH_2O) and destained with destain solution (50% methanol, 10 % acetic acid, and 40 % ddH_2O). Gels were stored in ddH_2O at room temperature.

Protein concentration quantification: BSA & densitometry

Protein concentration after purification was assessed by SDS-PAGE using bovine serum albumin (BSA) to create a standard curve on SDS-PAGE gels and comparing it to unknown quantities of our protein of interest, hLTC_4S, by densitometry. Densitometry quantifies protein loads by comparatively measuring the intensity of Coomassie Blue stain (Vincent *et al*., 1997). Using SDS-PAGE with BSA standards will reveal the total amount of protein recovered after expression and purification. It does not give any information as to what proportion is biologically active, so activity assays like ligand binding assays should be performed to determine the activity of the purified protein (Grishammer and Tate, 1995).

2.3 RESULTS AND DISCUSSION

Western blot of hLTC_4S

To confirm the purification and presence of hLTC_4S, a Western blow was performed, blotting against anti- hLTC_4S antibodies. Figure 2.3 displays the Western blot results.

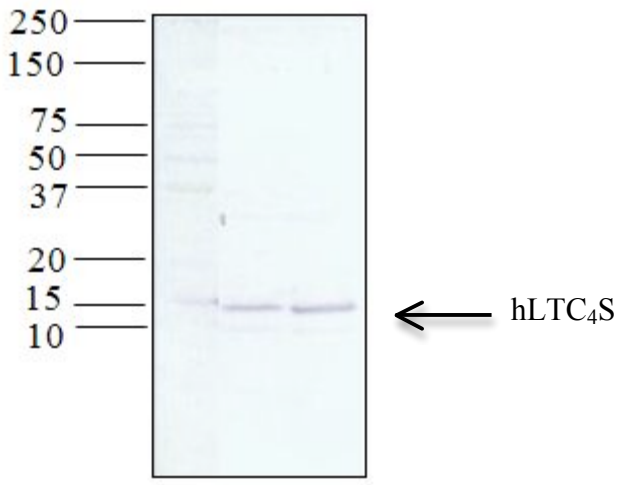

Figure 2.3. Western blot for $hLTC_4S$ detection. Western blot analysis identified the presence of target protein $hLTC_4S$ after IMAC purification.

Purification of $hLTC_4S$

The purification of $hLTC_4S$ was successfully reproduced following previously published methods from Schmidt-Krey *et al*. (2004), with slight modifications. Instead of purifying the protein using *S*-hexyl glutathione agarose for affinity chromatography, IMAC was employed to purify the C-terminal His_6-tagged target protein, following a final desalting step to help remove contamination proteins. This modified protocol is optimized because it allows for the purification of suitable amounts of protein, ~0.8 mg per liter of cell culture. From start to finish, the modified protocol can be performed in less than one day, and so exposes the MP to potentially denaturing detergents for short amounts of time, which could subsequently lead to the recovery of more stable purified protein. Also, after IMAC several high and low molecular weight contaminants are observed, including a 34, 27, 16, 14, and 6.5 kDa band. These contaminant bands are almost completely removed after buffer exchange, yielding > 90% purity for subsequent 2D crystallization trials (Figure 2.4). Buffer exchange was performed to change the purified proteins sitting buffer conditions, from the elution buffer to the desalting buffer

specifically removing the 300 mM imidazole and reducing the 0.5 M NaCl to 0.1 M concentration.

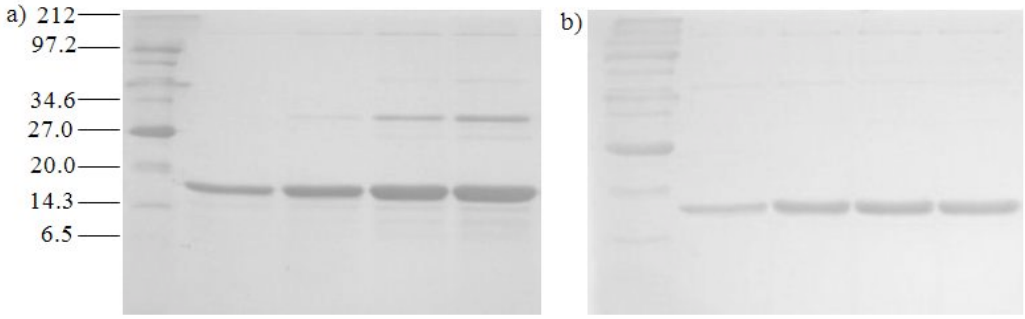

Figure 2.4. SDS-PAGE gels after after $hLTC_4S$ WT purification: before and after buffer exchange. Detergent solubilized $hLTC_4S$ was purified using two steps of column chromatography. A) First, IMAC was utilized to purify the C-terminal His_6-tagged $hLTC_4S$. B) Next, buffer exchange was performed to remove imidazole and NaCl from the buffer of the purified protein. After buffer exchange, several contaminants were almost completely removed, leaving a predominantly pure protein sample for 2D crystallization trials.

Protein samples were not boiled prior to SDS-PAGE analysis because MPs will aggregate irreversibly when heated, visibly precipitating inside the bottom of the gel well and not migrating towards the anode of the SDS-PAGE and so cannot be visibly detected on the gel (Dobrovetsky *et al*., 2007 and Yang *et al*., 2009).

2.4 CONCLUSIONS

The purification of both WT and mutant R104A $hLTC_4S$ was successfully reproduced using a modified version of a previously established protocol by Schmidt-Krey *et al*. (2004). The established protocol was modified to remove the *S*-hexyl glutathione agarose for affinity chromatography due to low purification yields, which most likely is a result of manufacturer inconsistencies. Instead IMAC and buffer exchange were employed to purify $hLTC_4S$. The modified purification protocol can be completed in less than one day, reducing the amount of time that target protein is exposed to potentially denaturing detergents. The target protein was purified to apparent homogeneity according to SDS-PAGE. ~0.8 mg of protein was purified per liter of starting cell culture, which is a sufficient concentration for 2D crystallization trials.

2.5 APPENDIX

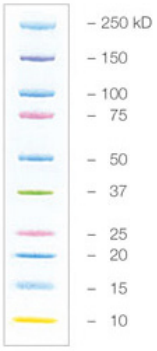

Figure B.1. Precision Plus Protein™ Kaleidoscope Standards.

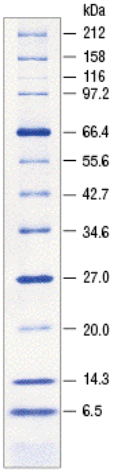

Figure B.2. New England BioLabs® Inc., Protein Marker, Broad Range (2 – 212 kDa)

2.6 BIBLIOGRAPHY

Abeyrathne, P.D., Chami, M., Pantelic, R.S., Goldie, K.N., Stahlberg, H., 2010. Preparation of 2D crystals of Membrane Proteins for High-Resolution Electron Crystallography Data Collection. *Methods in Enzymology* 481 (10), 81001 - 81008.

Ago, H., Kanaoka, Y., Irikura, D., Lam, B.K., Shimamura, T., Austen, K.F., Miyano, M., 2007. Crystal structure of a human membrane protein involved in cysteinyl leukotriene biosynthesis. *Nature* 448 (7153), 609 - 612.

Aveldano, M.I., 1995. Phospholipid solubilization during detergent extraction of rhodopsin from photoreceptor disk membranes. *Archives of Biochemistry and Biophysics* 324 (2), 331 – 343.

Banerjee, P., Joo, J.B., Buse, J.T., Dawson, G., 1995. Differential solubilization of lipids along with membrane proteins by different classes of detergents. *Chemistry and Physics of Lipids* 77 (1), 65 – 78.

Grishammer, R., and Tate, C.G., 1995. Overexpression of integral membrane proteins for structural studies. *Quarterly Review of Biophysics* 28 (3), 315 – 422.

Gaberc-Porekar, V. and Menart, V., 2001. Perspectives of immobilized-metal affinity chromatography. *Journal of Biochemistry and Biophysical Methods* 49 (1 – 3), 335 – 360.

Mosser, G., 2001. Two-dimensional crystallogenesis of transmembrane proteins. *Micron* 32 (5), 517 – 540.

Newby, Z., O'Connell III, J.D., Gruswitz, F., Hays, F.A., Harries, W.E., Harwood, I.M., Ho, J.D., Stroud, R.M., 2009. A general protocol for the crystallization of membrane proteins for x-ray structural investigation. *Nature Protocols* 4 (5), 619 - 637.

Noble, J.E. and Bailey, M.K.A., 2009. Quantitation of protein. *Methods in Enzymology* 463, 73 – 95.

Porath, J., 1992. Immobilized metal affinity chromatography. *Protein Expression and Purification* 3 (4), 263 – 281.

Seddon, A.M., Curnow, P., Booth, P.D., 2004. Membrane proteins, lipids and detergents: not just a soap opera. *Biochimica et Biophysical Acta* 1666 (1 – 2), 105 – 117.

Schmidt-Krey, I., Kanaoka, Y., Mills, D.J., Irikura, D., Haase, W., Lam, B.K., Austen, K.F., Kühlbrandt, W., 2004. Human leukotriene c4 synthase at 4.5 angstrom resolution in projection. *Structure* 12 (11), 2009 – 2014.

Vincent, S.G., Cunningham, P.R., Stephens, N.L., Halayko, A.J., Fisher, J.T., 1997. Quantitative densitometry of proteins stained with coomassie blue using a Hewlett Packard Scanjet scanner and scanplot software. *Electrophoresis* 18 (1), 67 – 71.

CHAPTER 3

3. TWO-DIMENSIONAL CRYSTALLIZATION OF HUMAN LEUKOTRIENE C4 SYNTHASE

3.1 BACKGROUND AND SIGNIFICANCE

Overview of previous work done for $hLTC_4S$

Structure-function studies of $hLTC_4S$ rely on previous work established on the enzyme. A brief description of the history of $hLTC_4S$ will be described. $hLTC_4S$ was first purified in 1992 from the KG-1 myeloid cell line. Microsomes were solubilized in 0.4% Na-DOC and 0.4% Triton X-102 following purification using an *S*-hexyl-glutathione agarose column (Penrose *et al*., 1992). Expression cloning of the cDNA for $hLTC_4S$, from the KG-1 cDNA expression library, was performed by Lam *et al*. (1994), revealing that $hLTC_4S$ belongs to the MAPEG family of proteins, which was first defined in 1999 (Jakobsson *et al.,*1999). The nucleotides of the $hLTC_4S$ gene were isolated and sequenced by Penrose *et al*. (1996) demonstrating that $hLTC_4S$ and FLAP are highly conserved. Functional characterization of $hLTC_4S$ was assessed by site-directed mutagenesis, focusing on shared and conserved amino acid residues between $hLTC_4S$ and FLAP. Specifically, these residues include Arg51, Tyr59, Tyr97, Tyr93, Asn55, Val49, Ala52, and Arg104. A putative mechanism for $hLTC_4S$ proposed Tyr93 activated the thiolate anion of GSH and Arg51 opened the epoxide of LTA_4 (Lam *et al*., 1997).

Oligomerization of functionally active $hLTC_4S$ has been the topic of debate for several years because various papers presented conflicting data: gel filtration chromatography suggested the presence of a homodimer (Nicholson *et al*., 1993), bioluminescence energy transfer proposed that $hLTC_4S$ forms a homooligomer (Svartz *et al*., 2003), and fluorescence energy transfer and crosslinking studies indicate that $hLTC_4S$ forms a hetero-dimer or hetero-trimer with FLAP (Mandal *et al*., 2004). The oligomerization of $hLTC_4S$ was first confirmed by Schmidt-Krey *et al.* in 2004. A

projection map, produced by electron crystallography of well-ordered 2D crystals at 4.5 Å resolution showed that $hLTC_4S$ crystallizes as a homotrimer with p321 symmetry (Figure 3.1). A projection map displays a three-dimensional body on a plane of two dimensions, which provides a top-down view of the protein. Projection densities revealed the presence of four transmembrane helices that run near perpendicular to the membrane. $hLTC_4S$ crystals form a lattice with plane group symmetry *p*321 with unite cell dimensions of a = b = 73.4 Å, $\gamma = 120°$. One $hLTC_4S$ monomer is about 20 by 22 Å in dimension, while a trimer is about 43 Å in diameter. This study confirmed for the first time how $hLTC_4S$ oligomerizes to form a functionally active enzyme (Schmidt-Krey *et al*., 2004).

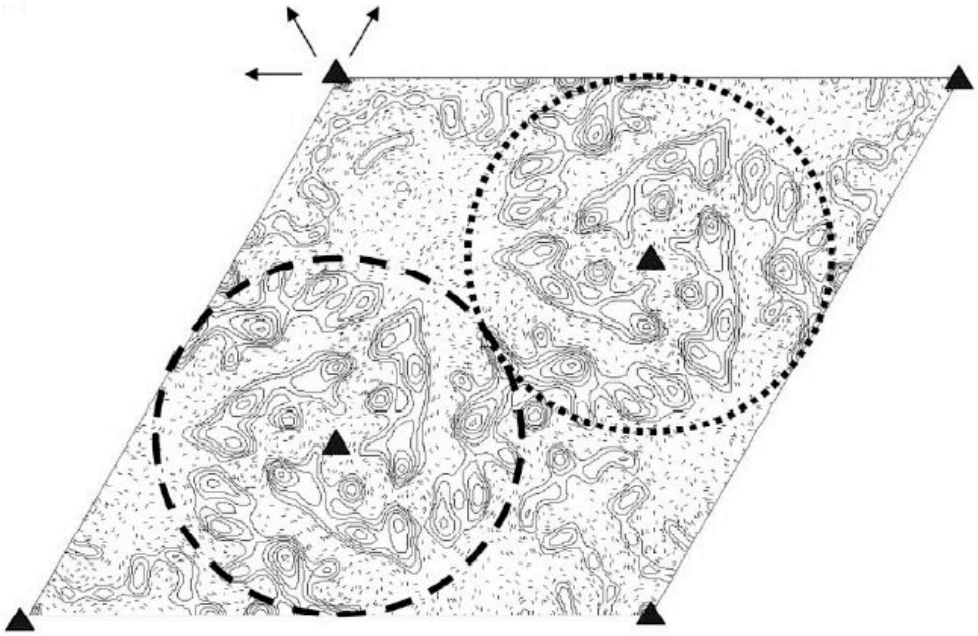

Figure 3.1. Projection map of $hLTC_4S$. Projection map of $hLTC_4S$ was solved by electron crystallography of 2D crystals. The projection map shows two trimers, circled by dashed and dotted lines, showing opposing membrane insertion orientations. Each trimer displays 12 circular densities, four per monomer. Two-fold axis indicated by arrows (Schmidt-Krey *et al*., 2004).

The 3D structure of $hLTC_4S$ was first solved in 2007 by two different groups (Ago et al., 2007 and Molina *et al*., 2007), both by x-ray crystallography. Ago *et al*. co-crystallized the enzyme with GSH to produce a 3D structure at 3.3 Å resolution. Molina *et al.* crystallized both the apo-enzyme and GSH-bound enzyme at 2.00 and 2.15 Å resolution, respectively. Both authors reported similar findings, which closely agreed with Schmidt-Krey *et al.* (2004). $hLTC_4S$ crystallizes as a homotrimer with threefold symmetry, where each monomer is composed of five α-helices. Helices I – IV are transmembranous and helix V is found in the perinuclear space (Figure 3.2). The GSH binding site revealed several amino acid residues that interact with the substrate, including Arg104 and Arg 31, which are of particular interest to the Schmidt-Krey lab.

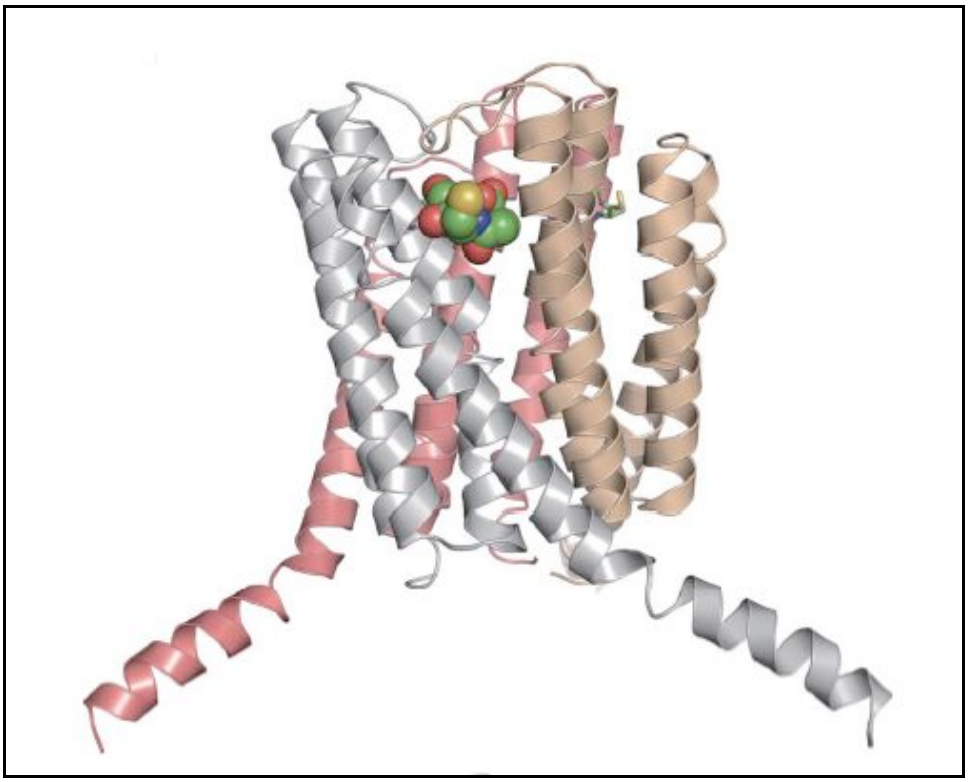

Figure 3.2. X-ray crystal structure of $hLTC_4S$ solved by x-ray crystallography to 3.3 Å resolution. The structure revealed a homotrimer, with each monomer composed of five α- helices, four of which are located within the membrane, and the final fifth helix protrudes into the perinuclear space. The three colored segments (grey, pink, and brown) represent monomers and one GSH molecule is shown in space-filling model, while the other two are shown in stick model (Ago *et al.,* 2007).

Electron crystallography of hLTC$_4$S

Electron crystallography is a developing field in structural biology, complementary and alternative to methods such as x-ray crystallography and nuclear magnetic resonance (NMR) spectroscopy, in the structural and functional studies of MPs. Electron crystallography relies on the growth and analysis of large, well-ordered two-dimensional crystals by electron microscopy (Kühlbrandt, 1992, Schmidt-Krey, 2007, and Abeyrathne *et al.,* 2010). The methods that first helped to develop the field of electron crystallography came from Richard Henderson and Nigel Unwin in 1975 with the structural determination of purple membrane, a MP that naturally forms 2D arrays (Henderson and Unwin, 1975), and which was further refined to atomic resolution in 1996 (Grigoriegg *et al.,* 1996). The first atomic-resolution structure was solved by x-ray crystallographic techniques by Johann Deisenhofer and Hartmut Michel of the Rhodopseudomonas viridis photosynthetic reaction center in 1985 (Deisenhofer *et al.,* 1985). A total of 308 unique structures of MPs have been solved to date (Figure 3.3) (White, 2009), most of which have been solved by x-ray crystallography. This is in stark contrast to the 80,000 + structures in the Protein Data Bank (PDB), most of which are of soluble proteins.

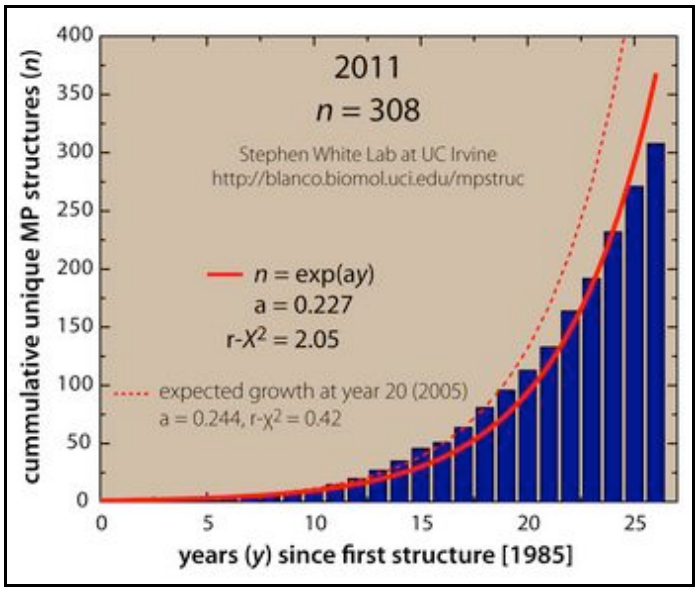

Figure 3.3. Progress in MP structure determination. The number of unique MP structures solved, since the first atomic-resolution structure of photosynthetic center in 1985, has grown tremendously. As of 2011, 208 unique MP structures have been solved, but this is in stark contrast to 80,000 + structures deposited in the PDB, which are mostly of soluble proteins (Http://blanco.biomol.uci.edu/mpstruc/listAll/list).

Structure determination by electron crystallography is advantageous because electron crystallography of 2D crystals is well-suited to study proteins in varying conditions (Kühlbrandt, 2012), such as pH-induced changes observed in sodium-proton antiporters NhaP and NhaA (Vinothkumar *et al.,* 2005 and Appel *et al*., 2009). Also, 2D crystals are composed of ordered MPs embedded within a continuous lipid bilayer, closely resembling what would be seen *in vivo*. Another benefit to 2D crystallization is that the MP is exposed to high concentrations of detergent only during the experimental portions of solubilization and purification, whereas in x-ray crystallography the target protein is exposed to detergents during the solubilization, purification and crystallization experiments, which may lead to protein instability (Abeyrathne *et al*., 2010). The major limiting factor for successful MP crystallization is the growth of large, well-ordered and thus diffraction quality crystals (Seddon *et al.,* 2004). For microsomal glutathione transferase 1 (MGST1) is was shown that slower crystallization rates resulted in the

growth of larger crystals that were related to the length of dialysis time (Schmidt-Krey *et al*., 1998). To date, only a handful of MP structures have been solved to greater than 4 Å resolution, including bacteriorhodopsin at 3.5 Å resolution (Kühlbrandt, 1994), aquaporin-1 at 3.7 Å resolution (Ren *et al.,* 2000), MGST1 at 3.2 Å resolution (Holm *et al.,* 2006) and aquaporin-0 at 1.9 Å resolution (Gonen *et al.,* 2005), which is the highest resolution 3D structure of a MP obtained by electron crystallography of 2D crystals to date.

There are several differences between electron crystallography and x-ray crystallography. Electron crystallography requires less protein as lower concentrations of purified protein, only 0.5 – 1 mg per mL (Ubarretxena-Belandia and Stokes, 2010), are required for systematic investigations of optimal crystallization parameters. It should be noted that 2D crystallization trials require a larger volume of purified protein than 3D crystallization requires, but still need less concentrated protein for 2D crystallizations. Screening of crystallization conditions requires that specimen be inspected individually by electron microscopy. In terms of size, 2D crystals are smaller and measure 0.5 – 5 μm or larger in diameter, whereas 3D crystals require a minimum size of 100 μm for x-ray diffraction. In terms of crystallization conditions, 2D crystal formation occurs at low to moderate ionic strength and neutral pH, whereas 3D crystal formation occurs at high ionic strength and slightly acidic and/or basic pH values (Abeyrathne *et al.,* 2010, Newby *et al.,* 2009). Electron crystallography and x-ray crystallography have one main step in common: the iterative pathway for structure determination, especially when in the crystallization phase of the experimental workflow. Once crystals have been grown, it can take anywhere from weeks to months to obtain well-ordered and large crystals, where within this time range parameters critical to crystal formation are adjusted in a step-wise and systematic manner to refine and optimize the conditions to maximize crystal size and quality (Newby *et al*., 2009). X-ray and electron crystallography can be combined to study MPs (Kühlbrandt, 2012). For example, if the x-ray structure of a homologous

protein is available, atomic models can be built as was done for NhaP1 (Goswami *et al*., 2011).

Electron crystallography of $hLTC_4S$ may reveal important structural information, as the protein is crystallized in lipid instead of detergent. There are still unanswered questions about the mechanism of product formation. How does $hLTC_4S$ conjugate two very different substrates, hydrophilic GSH and hydrophobic LTA_4? How does LTA_4 approach the enzyme active site, from above or within the membrane? There are difficult questions to tackle experimentally because LTA_4 is very unstable in solution.

Reconstitution of protein into a lipid bilayer

After detergent solubilization and purification of the target protein, which is obtained well beyond the CMC, excess detergent must be removed, in the presence of exogenous lipid, in order to reconstitute the MP into an artificial bilayer in solution (Abeyrathne *et al*., 2010). This can be obtained through a variety of techniques: dialysis, hydrophobic absorption, dilution, and the use of cyclodextrins (Kühlbrandt, 1992, Remigy *et al*., 2003, Signorell *et al*., 2007). Dialysis was used for $hLTC_4S$ reconstitution, therefore the later three methods will be described briefly. Hydrophobic absorption relies on the use of insoluble, hydrophobic "beads" that attract the hydrophobic tails of detergent molecules. After absorption, beads can be removed by centrifugation. Hydrophobic absorption is most successful at removing detergents with a low CMC (Seddon *et al*., 2004). The dilution method dilutes mixed protein, lipid and detergent solutions at known dilution factors. Dilution yields fairly reproducible results and is a method most recommended for high CMC detergents (Mosser, 2001). Finally, cyclodextrins are ring-shaped molecules with a non-polar ring environment that interact with detergents regardless of classification or CMC. Cyclodextrins do not interact with lipids because they have a higher affinity for detergent, and so do not affect reconstitution parameters (Abeyrathne *et al*., 2010).

Reconstitution of $hLTC_4S$ into a lipid membrane was achieved via dialysis, according to Schmidt-Krey *et al*. and Zhao *et al*. (Schmidt-Krey *et al*., 2004 and Zhao *et al.*, 2010). Dialysis is one of the most popular methods used to remove detergent from the detergent-solubilized purified protein solution. In this method, a ternary mixture of detergent, target protein, and lipid are combined and dialyzed against detergent-free buffer, within dialysis membranes with molecular weight cutoff (MWCO) large enough to allow the movement of detergent monomers out of the membrane but small enough to retain the target protein. The hydrophobic fatty acid chains of the lipid molecules strongly prefer to be in contact with the hydrophobic parts of the MP, while detergent monomers dissociate from the micelle-surrounded target protein at concentrations below their CMC. Lipid molecules begin to insert into the micelle, forming proteoliposomes. Lipid should be equilibrated with the detergent-protein mixture before detergent removal is attempted, because although detergent exchange between micelles is rapid, lipid molecules cannot move freely in aqueous solution (Kühlbrandt, 1992). Over a period of several days reconstitution of the target protein into a synthetic lipid bilayer will occur, forming 2D crystals (Seddon *et al.,* 2004 and Abeyrathne *et al*., 2010).

The dialysis method is more practical for detergents with a high CMC as the rate of dialysis is determined by the CMC of the detergent, with low CMC detergents dialyzing more slowly than high CMC detergents. This is potentially advantageous for detergents with low CMCs as the slow detergent removal rates may aid in the growth of well-ordered, large 2D crystals (Schmidt-Krey *et al.,* 1998). There are several examples of 2D crystal growth of MPs solubilized by low and high CMC detergents, followed by detergent removal via dialysis. These include MGST1 (Schmidt-Krey *et al*, 2000), NhaA (Williams, 2000), EmrE (Ubarretxenna-Belandia *et al.,* 2003), AQP-0 (Gonen *et al*., 2005) and NhaP1 (Goswami *et al*., 2011). Na-DOC is a high CMC detergent (0.08 – 0.25% w/v), but TX-100 is a low CMC detergent (0.015%). Dialysis exposes the detergent to an excess of detergent-free buffer, helping to bring it below its CMC so that

detergent micelles will dissociate into individual monomers, which can easily be removed by dialysis (Seddon *et al*., 2004).

2D crystals are composed of protein, lipid and sometimes detergent. 2D crystal formation is dictated by the interactions between these individual components. Upon detergent removal of the ternary detergent-protein-lipid mixture, the target protein can either insert into pre-formed lipid membranes or aggregate together. The formation of these 2D crystals is believed to occur in one of three different models: the one-, two-, or three-stage process (Kühlbrandt, 1992). In the three-stage model, lipid bilayer sheets of vesicles form as detergent is removed. Next, protein molecules insert into these membranes in random orientation and finally, the protein arranges itself in an ordered orientation onto a 2D lattice. The two-stage model describes the first two steps occurring simultaneously, and the one-stage model describes all three steps occurring simultaneously (Kühlbrandt, 1992).

Upon MP reconstitution for electron crystallography, two different crystal types can form: 2D crystals or stacked 2D crystals (Figure 3.4). 2D crystals are thin, and depending on the target protein, range from 50 – 200 Å in thickness. The formation of 2D crystals is dictated primarily by hydrophobic interactions, primarily between MP contact points. 2D crystals can present in different membrane morphologies such as planar sheets, vesicles or tubes. Rarely, crystalline patches can form in native membranes (Figure 3.4a) (Stoeckenius *et al.,* 1979). These 2D crystals contain protein facing one direction because the protein does not dissociate from the membrane for crystallization, and instead undergoes rearrangement. Vesicles are collapsed membranes that sometimes contain protein facing one direction (Figure 3.4b) or in alternating directions (not shown). Vesicles are energetically stable, as they do not have any open edges where hydrophobic portions of lipid or protein are exposed to the aqueous solution (Abeyrathne *et al*., 2010). Tubular crystals are elongated vesicles with protein arranged helically along the outer surface of the vesicle. Planar-tubular crystals are similar to

tubular crystals, but are wider in diameter. Planar-tubular crystals are more common after two-dimensional crystallizations and contain two crystal lattices. Figure 3.4c displays a cross-section of the tubular crystal. Sheets contain protein molecules embedded in alternating directions where energetically unstable edges of hydrophobic portions of lipid and protein are exposed t o aqueous solution (Figure 3.4d). Sometimes 2D crystals of sheets will stack upon each other, forming multilamellar crystals or thin 3D crystals. This is due in part to polar interactions like ionic strength and pH (Abeyrathne *et al.,* 2010). Figure 3.4e represents these thin 3D crystals, with protein molecules stacked exactly in register. Finally, it should be noted that 2D crystals limit protein freedom of movement in two dimensions, which should help improve the likelihood of lattice formation (Kühlbrandt, 1992).

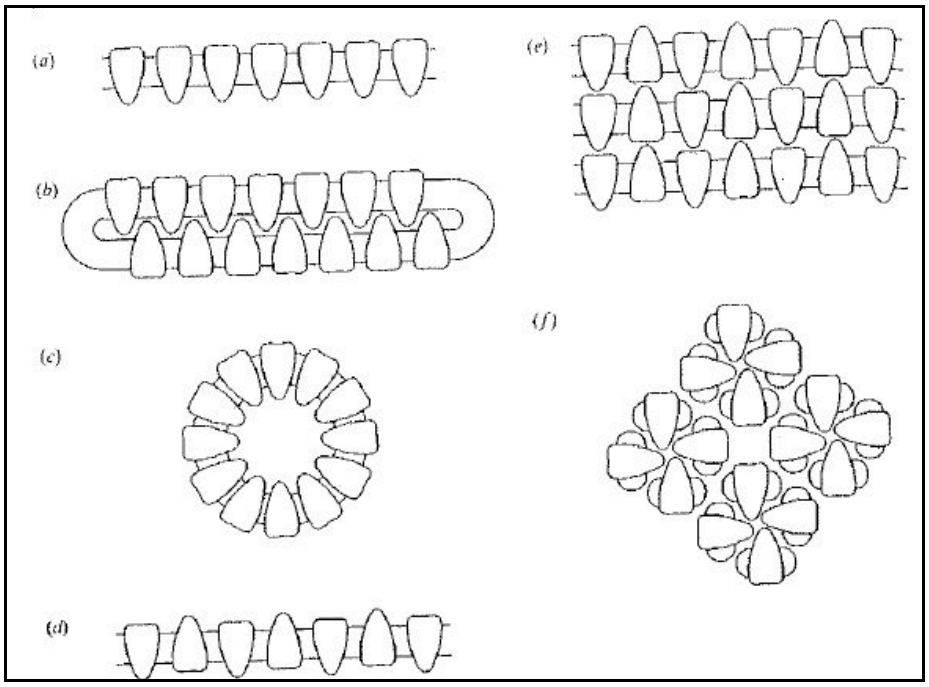

Figure 3.4. Membrane protein crystal types. After reconstitution, MPs can form three different types of crystals: 2D (a-d), 3D (f), and stacked 2D crystals (e). a) 2D crystals of native membrane and b) vesicles have protein insertion occur in the same direction. c) Elongated vesicles can form planar-tubular or tubular crystals. d) Typically seen after reconstitution experiments are 2D crystals with alternating protein insertion. These 2D crystals can stack to form thin 3D crystals (e). Finally, 3D crystals are grown for x-ray crystallography (f) (Kühlbrandt, 1992).

Lipid-to-Protein Ratio

Initial crystallization trials should systematically test a range of LPRs between 0 and 1 (w/w) (Mosser, 2001) or between 1 and 30 (mol/mol) (Schmidt-Krey *et al.* 2007). Ideally, protein reconstitution will occur over a range of LPR values (Gulik-Krzywiki, 1987). Upon the initial growth of 2D crystals, lowering the LPR can help improve crystallization (Schmidt-Krey *et al.,* 1998, Mosser, 2001, Schmidt-Krey *et al.,* 2004, Schmidt-Krey *et al.,* 2007). The ideal LPR for successful 2D crystal growth is small enough to promote crystal contacts and high enough to prevent protein aggregation (Schmidt-Krey *et al.,* 2007, Abeyrathne *et al.,* 2010). A starting population of pure

protein is ideal because as protein crystallization occurs, the presence of any existing contaminants may interfere with lattice formation (Kühlbrandt, 1992).

The lipid of choice for MP reconstitution is important for 2D crystallization (Ubarretxena-Belandia and Stokes, 2010). The length of the fatty acid tail influences overall fluidity and thickness of the bilayer.. Biological membranes consist of a wide range of phospholipid molecules including diacylglycerol lipids with fatty acid tails 16 or 18 carbon atoms long. Bilayers form when the cross section of the polar head group and hydrophobic fatty acid tails are roughly the same size. If the head group is larger, micelle formation is common; if the head group is smaller, inverted micelles can form (Kühlbrandt, 1992). 1,2-dimyristory-*sn*-glycero-3-phosphocholine (DMPC) was selected for the reconstitution of $hLTC_4S$. DMPC is a lipid with less than the ideal 16 or 18 carbon atom fatty acid tail length. Instead, DMPC is a saturated synthetic lipid with 14 carbon atom chain length, a zwitterionic phoscholine (PC) head group, and a phase transition temperature of 23°C. The phase transition temperature refers to the temperature at which a rigid, lamellar bilayer transitions to a rigid, crystalline phase. Crystallization usually, but not always (Schmidt-Krey *et al.,* 2007), occurs at temperatures above the phase transition temperature (Kühlbrandt, 1992). Although DMPC has a shorter fatty acid chain length, it forms bilayers of 35 Å hydrophobic thickness, similar to the 35 Å hydrophobic center of a biological lipid bilayer. DMPC has been employed in the 2D crystallization of several MPs including photosystem I (Karrasch *et al.,* 1996), photosystem II (Tsiotis *et al*., 1996), MGST1 (Schmidt-Krey *et al.,* 2000), porin OmpF (Signorell *et al*., 2006), and human vitamin K-dependent γ-glutamyl carboxylase (Schmidt-Krey *et al*., 2007).

After MP reconstitution into a lipid bilayer, potential 2D crystals must be screened using an electron microscope, as 2D crystals are too small to view by light microscopy. In general, screening and detection of 2D crystallization trials is performed by negative stain of post-dialysis samples (Kühlbrandt *et al*., 1994). Due to the natural

low contrast observed in biological specimen, negative stain is used to provide high contrast of the specimen. Negative stains are heavy metal compounds. Non-uniform sample staining can result in the appearance of high contrast specimen in one area, and featureless regions in another area, which should be taken into account during screening of 2D crystals (Kühlbrandt, 1992).

3.2 MATERIALS AND METHODS

Materials

DMPC was purchased from Avanti® Polar Lipids, Inc. in 1 mg and 10 mg concentrations (lot # 140PC-254). The Spectra/Por® Dialysis Membrane 2 with a molecular weight cutoff (MWCO) of 12,000 – 14,000 Da and the Spectra/Por® closures were both purchased from Spectrum® Labs. Reagents for dialysis include HEPES purchased from Angus® Chemical Company, glycerol biotechnology grade from Amresco®, 2-mercaptoethanol (2-ME) from OmniPur®, ethylenediaminetetraacetic acid (EDTA) from Fisher Bioreagents®, L-glutathione reduced 97% (GSH) from Alfa Aesar®, and potassium chloride (KCl) from Acros®. Materials for electron microscopy include 400 mesh TEM regular grids (Cu, 3mm), purchased from SPI® Supplies, uranyl acetate dehydrate from Ted Pella, Inc., and muscovite mica V-5 from Electron Microscopy Sciences.

Methods

Activity Assays

In order to confirm that the protein is enzymatically functional, activity assays of the detergent solubilized protein and the post-dialysis samples were performed according to Lam *et al.* (1997). Activity assays were performed by our collaborating lab (Bing K. Lam, Department of Medicine Brigham and Women's Hospital, Boston). $hLTC_4S$

activity is measured by reverse phase high-performance liquid chromatography (RP-HPLC) assessing LTC_4-ME formation. Purified protein is incubated at room temperature along with GSH and LTA_4-Me. The enzymatic reaction is stopped by the addition of methanol and water. Prostaglandin B_2 (PGB_2) is added as an internal standard prior to RP-HPLC. LTC_4 is quantitated by the ratio of the LTC_4 peak compared to the PGB_2 internal standard.

Protein reconstitution: dialysis setup

The lipid was solubilized in Na-DOC, according to Schmidt-Krey *et al.* (Schmidt Krey *et al.,* 1998 & 2000): 1,2-dimyristoyl-sn-glycero-3-phosphocholine (DMPC), stored in chloroform, is carefully transferred to a round bottom flask. The chloroform is evaporated under a gentle stream of nitrogen gas. After chloroform evaporation, 0.5% Na-DOC is added to solubilize the dried lipid, sonicated for 5 minutes and stored at -20°C.

The 2D crystallization of $hLTC_4S$ was performed according to Schmidt-Krey *et al*. and Zhao *et al*. (Schmidt-Krey *et al.,* 2004 and Zhao *et al*., 2010). Exogenous lipid DMPC is added to the purified protein (see LPR Calculation). Rest on ice for 30 minutes and then pipette the ternary mixture of detergent-protein-lipid to an 8-cm long section of 1 cm flat width dialysis tubing (MWCO 12,000 – 14,000 Da). Dialyze against 250 mL of detergent-free dialysis buffer (50 mM HEPES, pH 7.6; 20% glycerol, 1 mM EDTA, 10 mM 2-mercaptoethanol, 10 mM GSH and 50 mM KCl) for 3 – 8 days at 23°C.

LPR determination

The lipid-to-protein ratio (LPR) defines the amount of lipid added to a solubilized protein solution for reconstitution to occur. The LPR was the main experimental variable that was adjusted during 2D crystallization trials of $hLTC_4S$, with a focus on

reconstitution at lower LPR ranges. The LPR values stated below are all molar values, unless otherwise stated. The calculation for LPR (mol/mol) is as follows:

$$LPR = n_{lipid}/n_{protein} = [(C_{lipid} * V_{lipid}) / MW_{lipid}] \div [(C_{protein} * V_{protein}) / MW_{protein}] \text{ (eqn 1)}$$

Eqn 1 describes the calculation for LPR (mol/mol) determination, where n = number of molecules, C = concentration (mg/mL), V = volume (mL) and MW = molecular weight (Da). A sample LPR (mol/mol) calculation can be seen below for a dialysis setup using 100 µL of $hLTC_4S$, purified to 0.8 mg/mL, using 1 mg/mL DMPC, and solving to a final LPR of 10:

$$10 = [(1 \text{ mg/mL} * V_{lipid}) / 678.15 \text{ Da}] \div [(0.8 \text{ mg/mL} * 100 \text{ µL}) / 50{,}000 \text{ Da}]$$

$$V_{lipid} = 10.8 \text{ µL}$$

The calculation for LPR (w/w) is as follows:

$$LPR = w_{lipid}/w_{protein} = (C_{lipid} * V_{lipid}) \div (C_{protein} * V_{lipid}) \text{ (eqn 2)}$$

Eqn 2 describes the calculation for LPR (w/w) determination, where w = weight (mg), C = concentration (mg/mL) and V = volume (mL).

Grid preparation of 2D crystals

After 3 – 10 days the sample is removed from dialysis for grid preparation. Any remaining post-dialysis sample is flash-frozen in LN_2 and stored at -80°C. 2D crystallization conditions of $hLTC_4S$ are screened by electron microscopy. 2D crystals

are stained with 1% uranyl acetate on a carbon coated copper 400 mesh grid. The grid is stored in a grid storage box and placed inside a desicator cabinet.

Screening 2D crystals by electron microscopy

Post-dialysis samples were negatively stained with uranyl acetate. 2D crystals were screened using a JEM-1400(JEOL® Ltd.) transmission electron microscope (TEM) with 120 kV accelerating voltage, equipped with Gatan Orius SC1000 and Ultrascan 1000 charge-coupled device (CCD) cameras. Images of membranes and 2D crystals were obtained at magnifications ranging from 25K (Gatan Orius SC1000) to 50K (Ultrascan 1000 CCD camera).

3.3 RESULTS AND DISCUSSION

Activity assays for $hLTC_4S$

The activity of $hLTC_4S$ was measured after two experimental steps: after purification (before dialysis) and after dialysis (Table 3.1). $hLTC_4S$ showed no activity after purification. This represents the detergent solubilized and purified protein. This result is not surprising as $hLTC_4S$ solubilization and purification requires the utilization of excess detergent, which is possibly denaturing. $hLTC_4S$ was solubilized in 1% TX-100 (CMC = 0.015% v/v) and 0.5% Na-DOC (CMC = 0.08 – 0.25% w/v), about 67X and 3X in excess to their CMC, respectively. The lack of enzymatic activity prior to 2D crystallization trials is not ideal, but what is more surprising and ultimately more important, is that $hLTC_4S$ activity after dialysis was high. This displays the critical importance of reconstitution with added exogenous lipid for enzyme activity. Also, greater activity was seen with the high LPR value in the post-dialysis samples, possibly suggesting that increased activity may be the result of reconstituted 2D crystals. This

LPR range, between 10 and 15, was shown to produce sheets and stacked 2D crystals, respectively. This is discussed in further detail below.

Table 3.1. Activity assays of hLTC$_4$S. Enzymatic activity, assessed by the production of LTC$_4$-Me, was measured for 2 sets of samples: pre-dialysis and post-dialysis. The pre-dialysis samples, which simply represent a population of detergent solubilized and purified proteins, showed no activity. However, the post-dialysis samples, which represent a population of purified protein after detergent removal and reconstitution into a lipid bilayer, showed high activity. This is due in part to the denaturing effects of high concentrations of detergents and also the essential nature of lipid for hLTC$_4$S activity.

Sample	Concentration	LPR	LTC4S activity (µmol/min/mg)
E1- pur	0.08 mg/mL	n/a	0.00
E2- pur	"	n/a	0.00
E1- dialysis	"	1	19.08
E2- dialysis	"	10	38.55

2D crystals of hLTC$_4$S WT

The main parameter that was varied during 2D crystallization trials of hLTC$_4$S was the lipid-to-protein ratio (LPR). It has been reported that careful selection of eluted protein fractions (instead of using batch and/or pooled purification elutions) and the LPR were critical factors that determined the success of 2D crystallization trials (Zhao *et al*., 2010). Following these guidelines, the LPR was again systematically tested for the growth of 2D crystals. Additionally, time in dialysis was found to yield interesting results, such as the growth of 2D crystals after only 3 days in dialysis, and so was added to the list of varied parameters in this study. Overwhelmingly, the most common membrane morphology that was obtained after dialysis of hLTC$_4$S was the growth and formation of stacked 2D sheets (Figure 3.5), varying from 0.1 – 10 µm in size. Within these stacked sheets a visible 2D lattice(s) was observed, that varied with LPR and time in dialysis (Table 3.2).

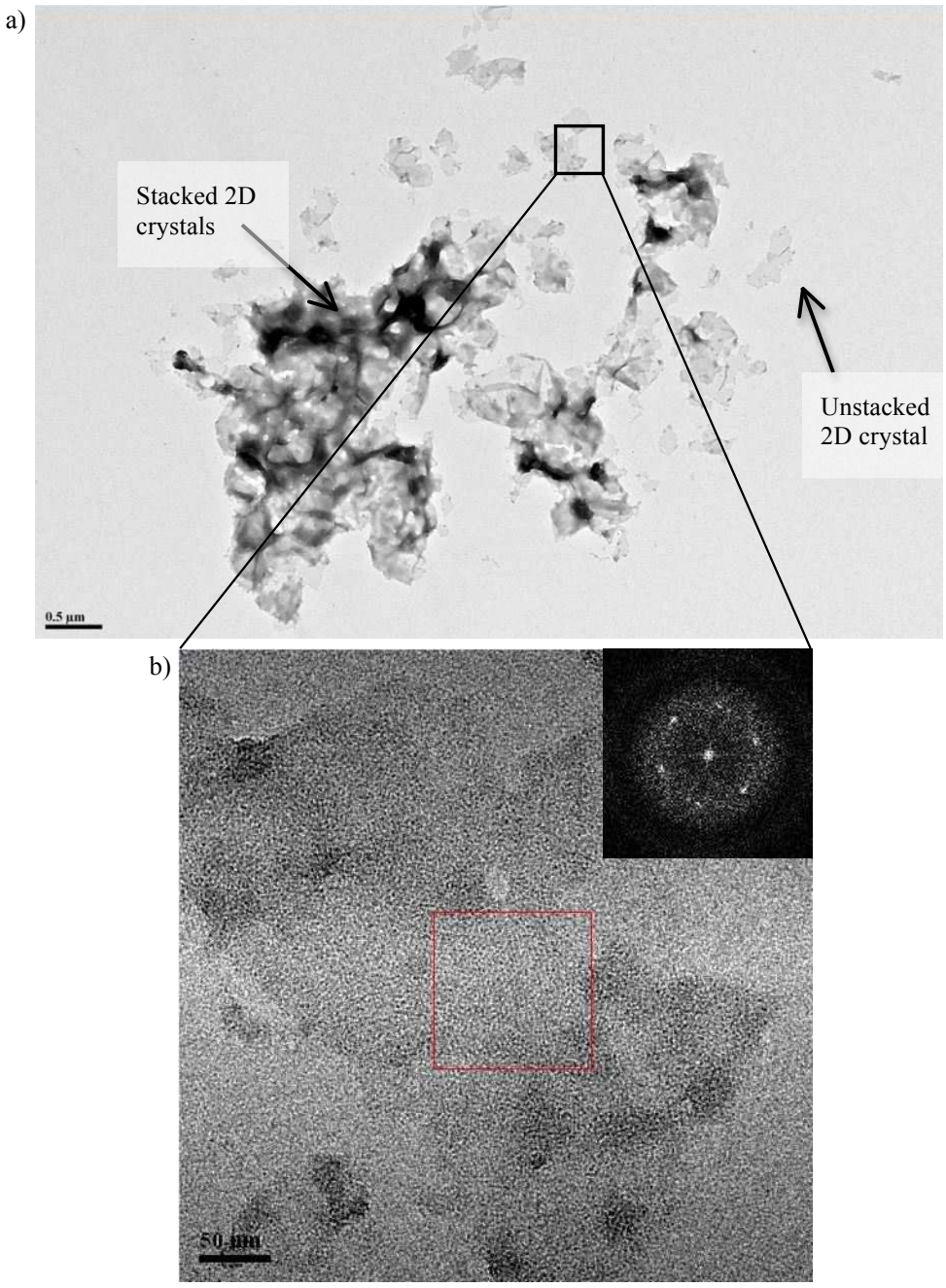

Figure 3.5. Stacked 2D crystals formation of hLTC$_4$S WT after 8 days in dialysis.. a) Low-magnification micrograph of negatively stained hLTC$_4$S. Sheets 0.1 – 1 µm in width are observed. Areas with single and multiple layers of membranes are apparent. b) High-magnification micrograph of boxed area in a). 2D crystalline lattice is visible, ~100 nm in width. Fast Fourier transform (FFT) of boxed area (red) inset displays six sharp spots. The spots of an FFT encode for the amplitude and phase of the protein structure (Abeyrathne *et al.,* 2010)

Table 3.2 2D crystallization parameters of $hLTC_4S$ WT. Variation of two conditions (LPR and time in dialysis) yielded substantially different results. The table below shows the experimental variation of LPR only, holding time and elution fractions consistent.

Purific-ation #	Elution	Conc (mg/mL)	LPR (mol/mol)	LPR (w/w)	Time in dialysis (days)	Results
56	E1	0.10	0	0	8	Aggregated protein
56	E1	0.10	5	0.067	8	Aggregated protein
56	E1	0.10	10	0.135	8	Sheets; no order
56	E1	0.10	15	0.202	8	Stacked sheets; crystals
56	E2	0.23	0	0	8	Aggregated protein
56	E2	0.23	5	0.067	8	Aggregated protein
56	E2	0.23	10	0.135	8	Aggregated protein
56	E2	0.23	15	0.202	8	Stacked sheets; crystals

Overall, 2D crystallization trials of $hLTC_4S$ followed the general rules of LPR-dependent 2D crystal growth (Figure 3.6) (Schmidt-Krey *et al.,* 2004, Zhao *et al.,* 2010). At low LPR ranges, between 0 – 5, protein aggregation was observed (Figure 3.6a). At high LPR ranges, between 6 – 15 (Figure 3.6a and 3.6b), a variation between sheets and stacked sheets were observed.

a)

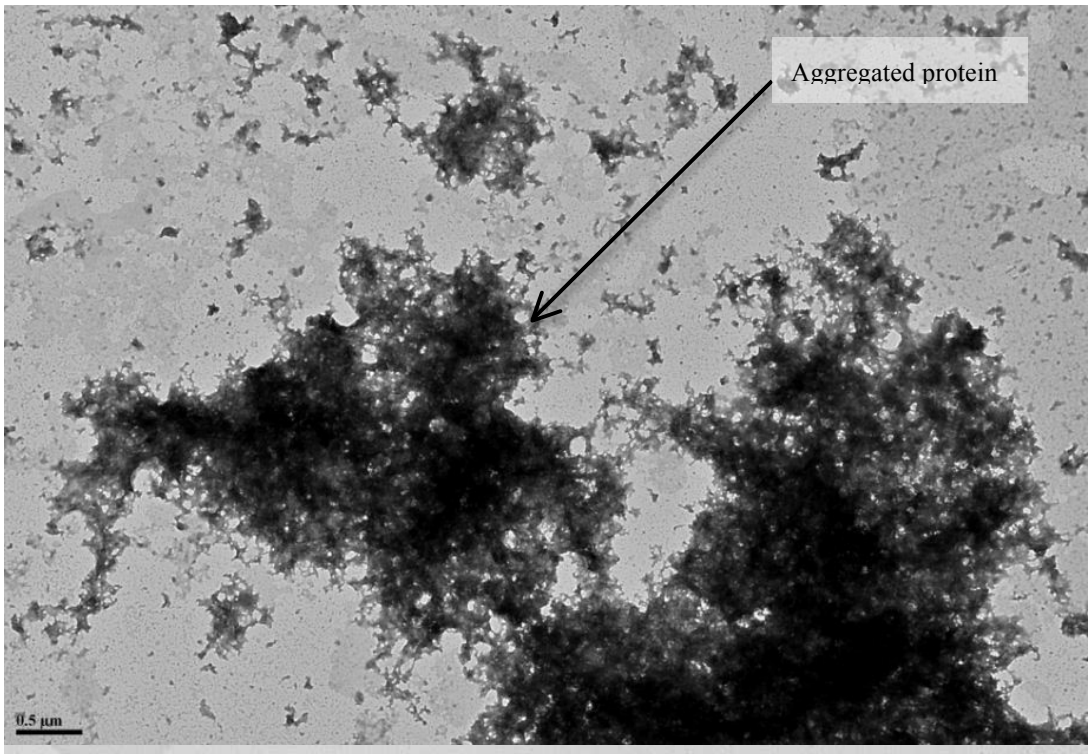

b)

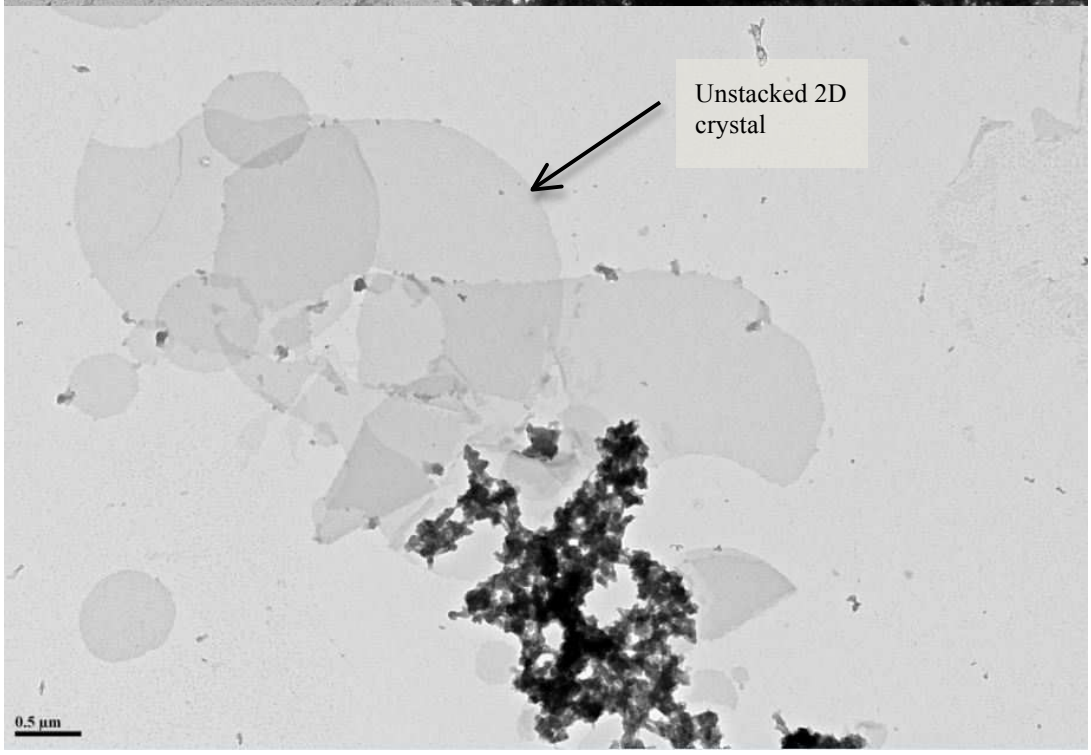

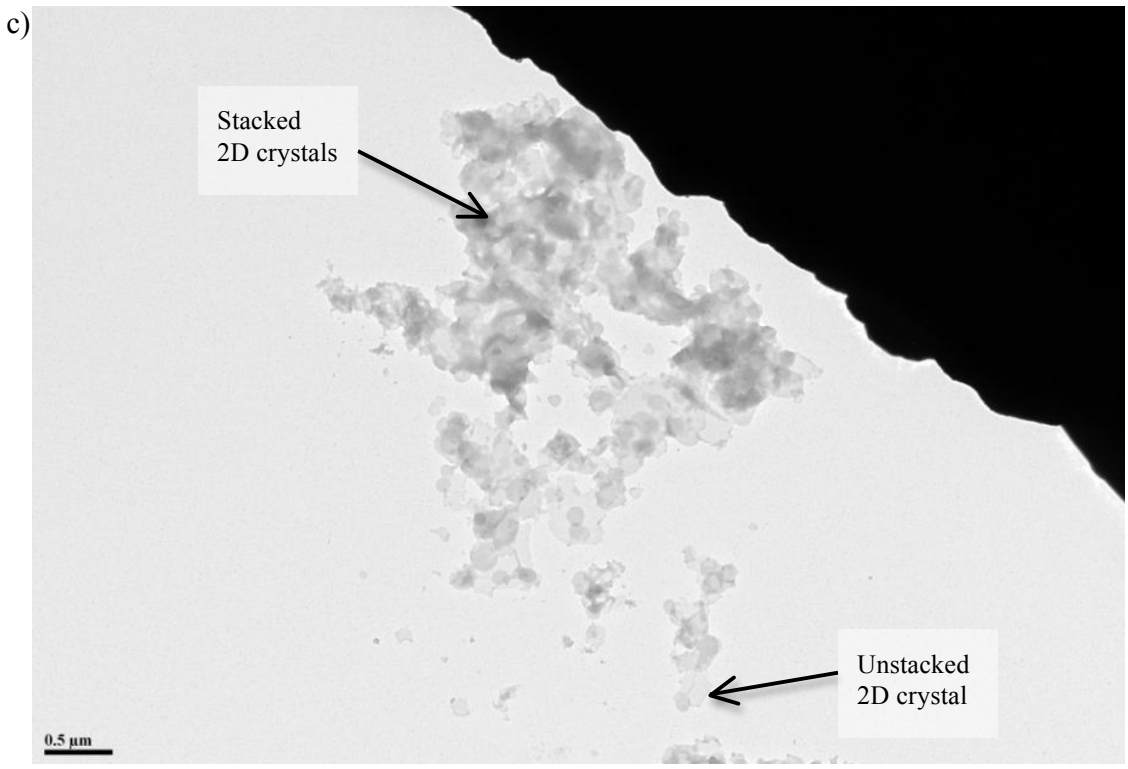

Figure 3.6. LPR-dependent 2D crystallization of $hLTC_4S$. a) At low LPRs, from 0 – 5, protein aggregation was observed, b) at LPR 10 sheets were seen, and c) at high LPRs of 15, stacked sheets were observed.

Stacked 2D crystals sometimes exist as a combination of in-plane hydrophobic interactions and hydrophilic interactions between lateral sheets. One explanation for the occurrence of stacked sheets is the presence of hydrophilic interaction between cytosolic loop portions connecting transmembrane segments. This is common especially when the target protein has large extramembranous domains. Crystal stacking is undesired because electrons interact with matter 10,000X more strongly than x-rays, emphasizing the need for extremely thin specimen. Although the stacks of 2D crystals are relatively thin, they are in precise register making it difficult to analyze and combine data collected from

tilted specimen. Tilting specimens of thin 2D stacks does not provide useful information for three-dimensional structure analysis (Kühlbrandt, 1992).

There are several examples of stacking of 2D sheets upon reconstitution. Cytochrome reductase, solubilized in TX-100, was crystallized using two different detergent removal methods: adsorption using polystyrene beads (Wingfield *et al.,* 1979) and dialysis (Hovmöller *et al.,* 1983). Adsorption by polystyrene beads yielded 2D crystals while dialysis led to the growth of stacked, multilamellar crystals. But it should be noted that the dialysis method was easier to control because the low CMC of TX-100 led to slower detergent removal rates and produced crystals up to 20 μm in size. In the second example, photosystem II (PS-II) reaction center, solubilized in dodecyl maltoside and reconstituted in buffer containing 200 mM $MgCl_2$ and 1.5% taurine yielded stacked 2D crystals (Dekker *et al.,* 1990, Boekema *et al.,* 1990). This may be due to the increased ionic strength of the buffer, or because taurine has ampiphilic properties, supporting 2D crystal formation (Dekker *et al.,* 1990 and Boekema *et al*., 1990). Finally, Ca^{+2} –ATPase formed stacked 2D crystals at a molar LPR of 25 (Figure 3.7). These thin 3D crystals measured several μm in diameter and contained stacked 2D crystals in register. The edge of stacked layers can be seen at the arrowheads. Stacking could be a result of the large soluble domains of Ca^{+2} –ATPase, which would increase the hydrophilic interactions between thin 2D crystals (Stokes and Green, 1990).

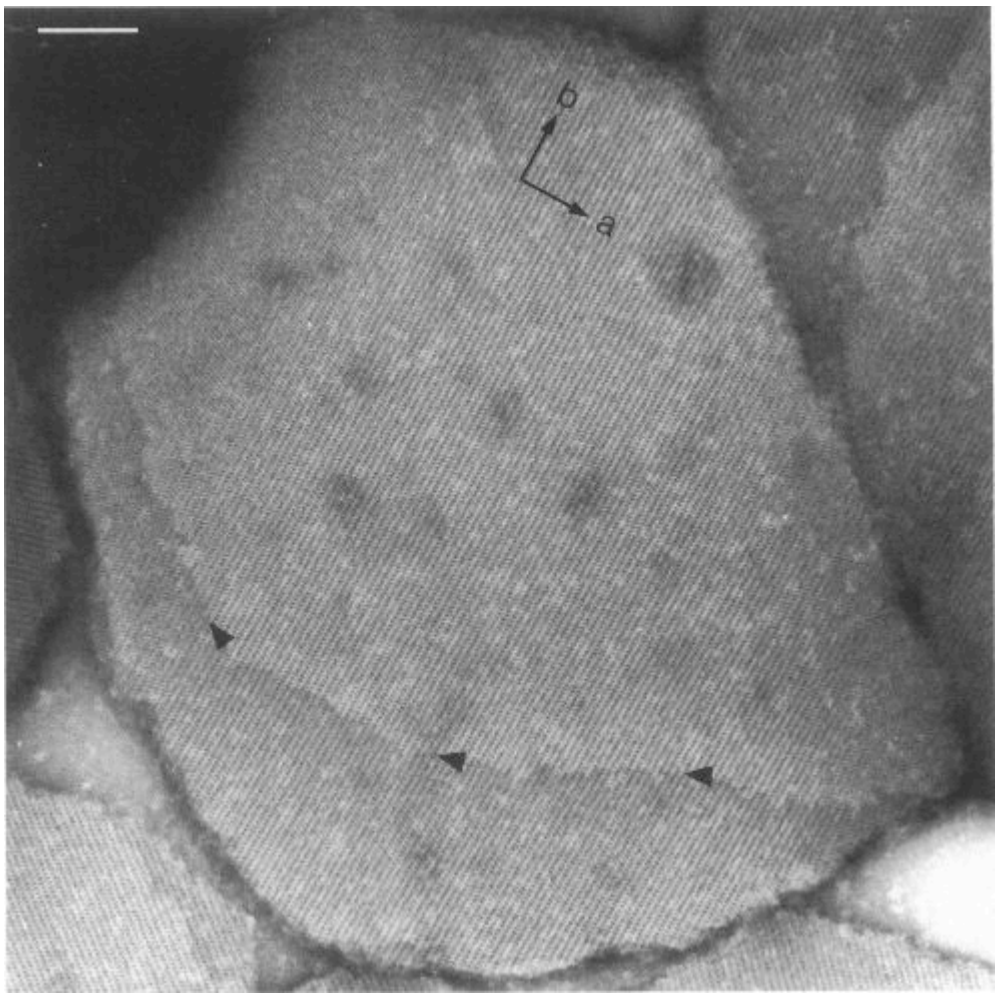

Figure 3.7. Stacked 2D crystals of Ca^{+2} –ATPase. Thin 3D crystals of Ca^{+2} –ATPase obtained at a molar LPR of 25. Edges of 2D crystals can be seen at the arrowheads. Scale bar = 0.1μm (Stokes and Green, 1990).

The formation of mosaic 2D crystals ~100 nm in size, after only 3 days in dialysis was surprising (Figure 3.8). Stacked sheets 0.1 – 2 μm in size were observed in most post-dialysis samples and even one sample contained sheets > 10 μm in the longest dimension (Figure 3.9). The rate of detergent removal is dependent on the CMC of the individual detergent used. TX-100 is a low CMC detergent and Na-DOC is a high CMC detergent. The Na-DOC, which has a small micellar weight of ~2,000 Da, is most likely dialyzed out of the protein solution quickly. This leaves TX-100, which has a large

micellar weight of ~90,000 Da to remain in the dialysis membrane with the protein in solution. One possible explanation for crystal formation in such short dialysis time is that a large portion, but not in its entirety, of TX-100 is already dialyzed out of solution in 4 days, observed by lab member (unpublished observation from Matthew Johnson). Overall, most studies have found that removal of Triton X-100 required 7 – 21 days (Schmidt-Krey *et al.,* 1999, Holm *et al.,* 2006, Jegerschold *et al.,* 2008, Zhao *et al.,* 2010).

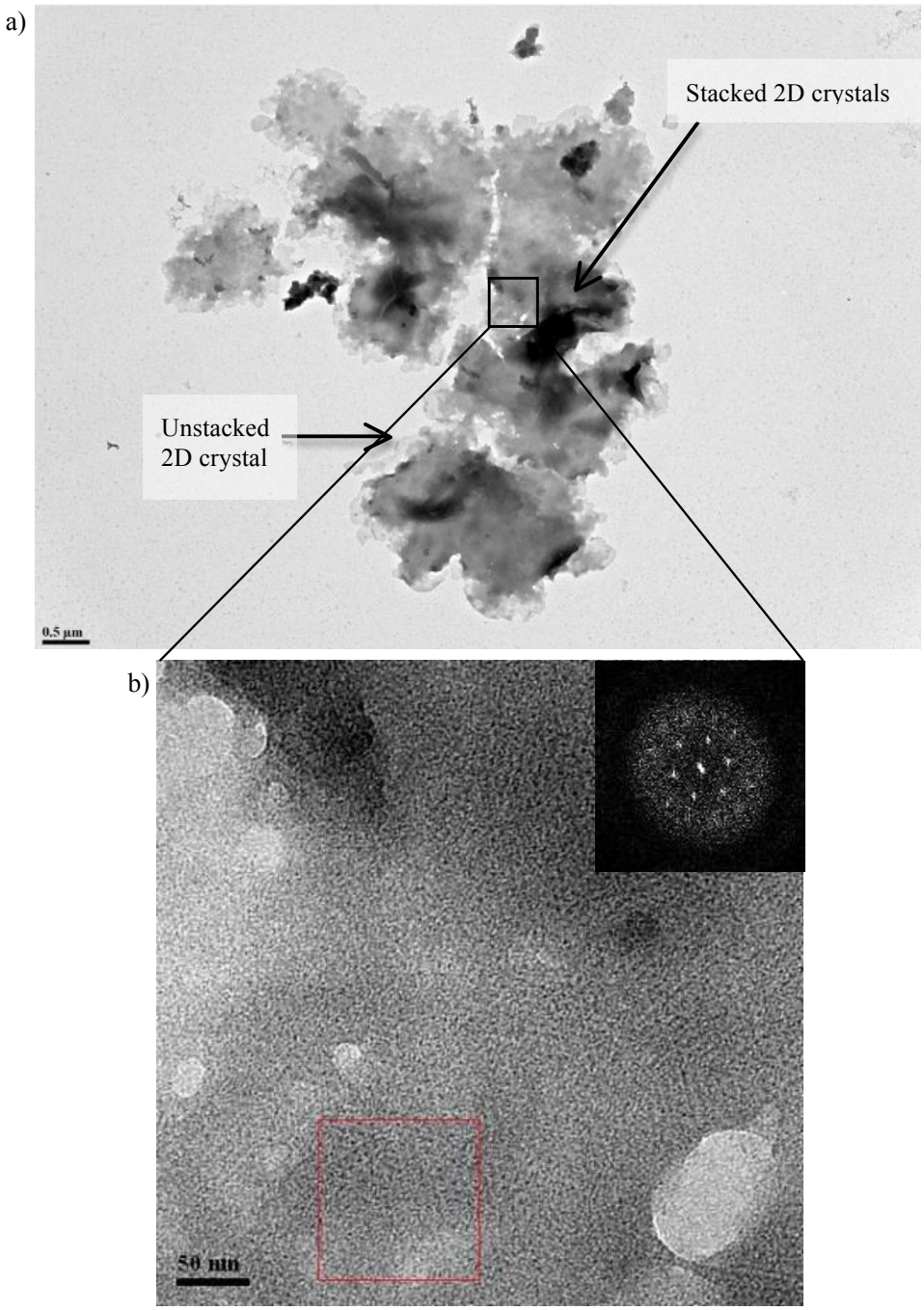

Figure 3.8. Stacked 2D crystals of hLTC$_4$S WT after 3 days in dialysis. The formation of stacked 2D crystals, at a molar LPR of 15 after only 3 days in dialysis was unexpected. The rate of detergent removal by dialysis is determined by detergent CMC, and thus the removal of low CMC TX-100 should be slow, although membranes were still obtained at this time point. a) Low-magnification micrograph of negatively stained hLTC$_4$S. Sheets 0.1 – 2 µm in width were observed. b) High-magnification micrograph of boxed area in a). Mosaic 2D crystalline lattice is visible, at least 100 nm in size. FFT of boxed area (red) inset.

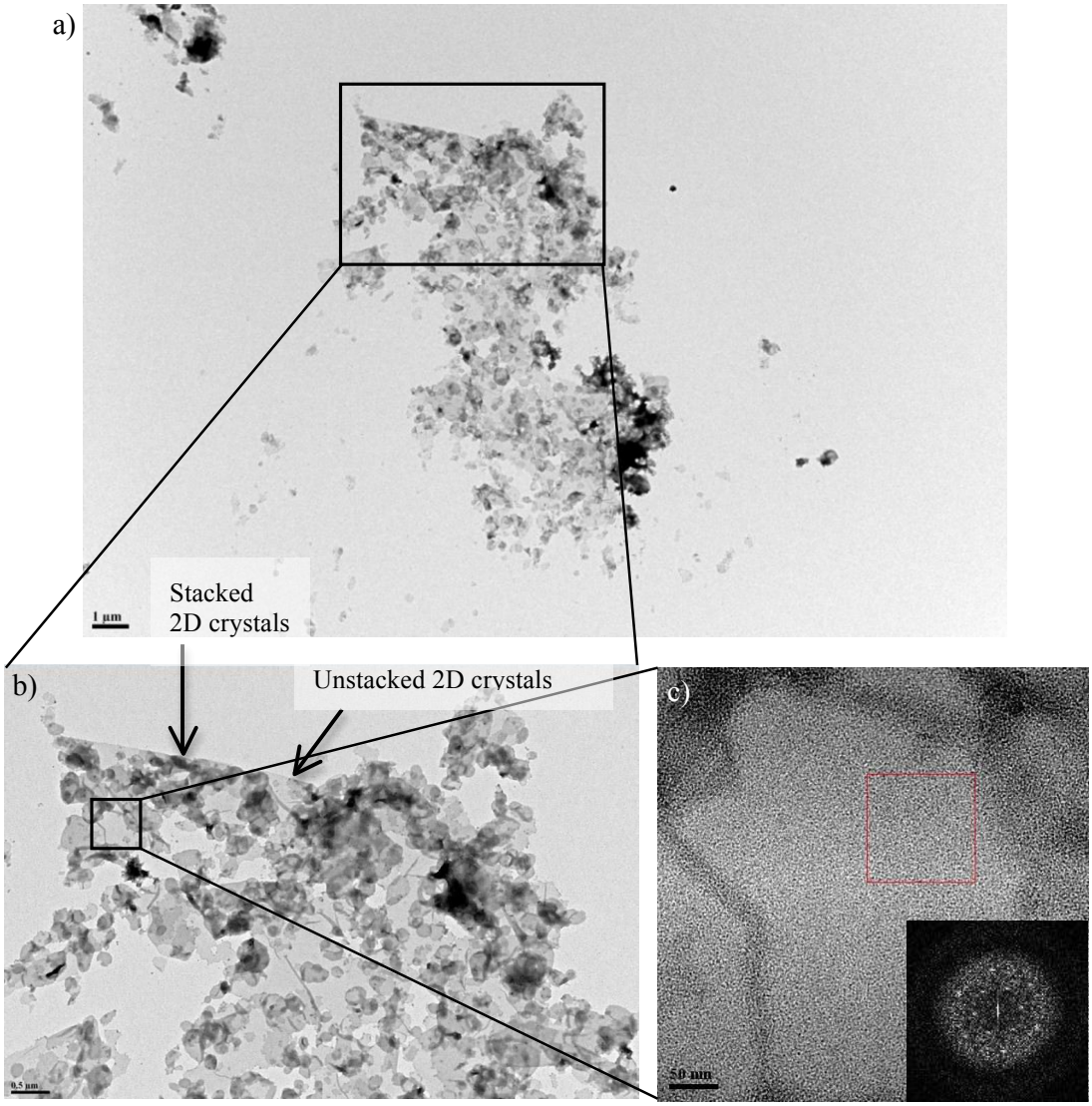

Figure 3.9. Large stacked sheets obtained after 3 days in dialysis. A large sheet >10 µm in the longest direction was observed after only 3 days in dialysis. The protein was purified to 0.22 mg/mL concentration. Reconstitution occurred at LPR 15. a) Low-mag micrograph of negatively stained hLTC$_4$S. b) Smaller sheets ~0.25 µm are seen stacked upon the larger 10 µm sheet. c) There are visibly apparent areas of single, unilamellar 2D sheets. Within unilamellar sheets, a visible 2D lattice is hardly ever observed. FFT analysis (inset) of the boxed area (red) shows the presence of crystalline patches.

2D crystals of hLTC$_4$S mutant R104A

Based on the mostly successful reproduction of methods to crystallize hLTC$_4$S WT (Schmidt-Krey *et al*., 2004 and Zhao *et al*., 2010), 2D crystallization trials of mutant R104A were performed following these previously established methods. 2D crystal growth followed similar patterns as was observed for WT (Table 3.3). R104A mutant was reconstituted into a lipid bilayer and formed stacked 2D crystals, similar to that seen for WT at LPR 15 (Figure 3.10). Encouragingly, minimally stacked sheets were also observed (Figure 3.11). FFT analysis suggests the presence of crystals, indicated by the weak spots observed (Figure 3.11b inset). These near-single layered crystals are ideal for further study by cryo-EM as these membrane morphologies are usually highly ordered under cryo conditions.

Table 3.3. 2D crystallization parameters of hLTC$_4$S mutant R104A. Variation of two conditions (LPR and time in dialysis) yielded substantially different results. The table below shows the experimental variation of LPR only, holding time in dialysis constant.

Purifi-cation #	Elution	Conc (mg/mL)	LPR (mol/mol)	LPR (w/w)	Time in dialysis (day)	Results
5	E2	0.213	0	0	8	Aggregated protein
5	E2	0.213	5	0.07	8	Aggregated protein
5	E2	0.213	10	0.135	8	Sheets; weak spots
5	E2	0.213	15	0.20	8	Sheets; weak spots
5	E4	0.462	0	0	8	Aggregated protein
5	E4	0.462	5	0.07	8	Aggregated protein
5	E4	0.462	10	0.135	8	Stacked sheets; no spots
5	E4	0.462	15	0.20	8	Stacked sheets; crystals

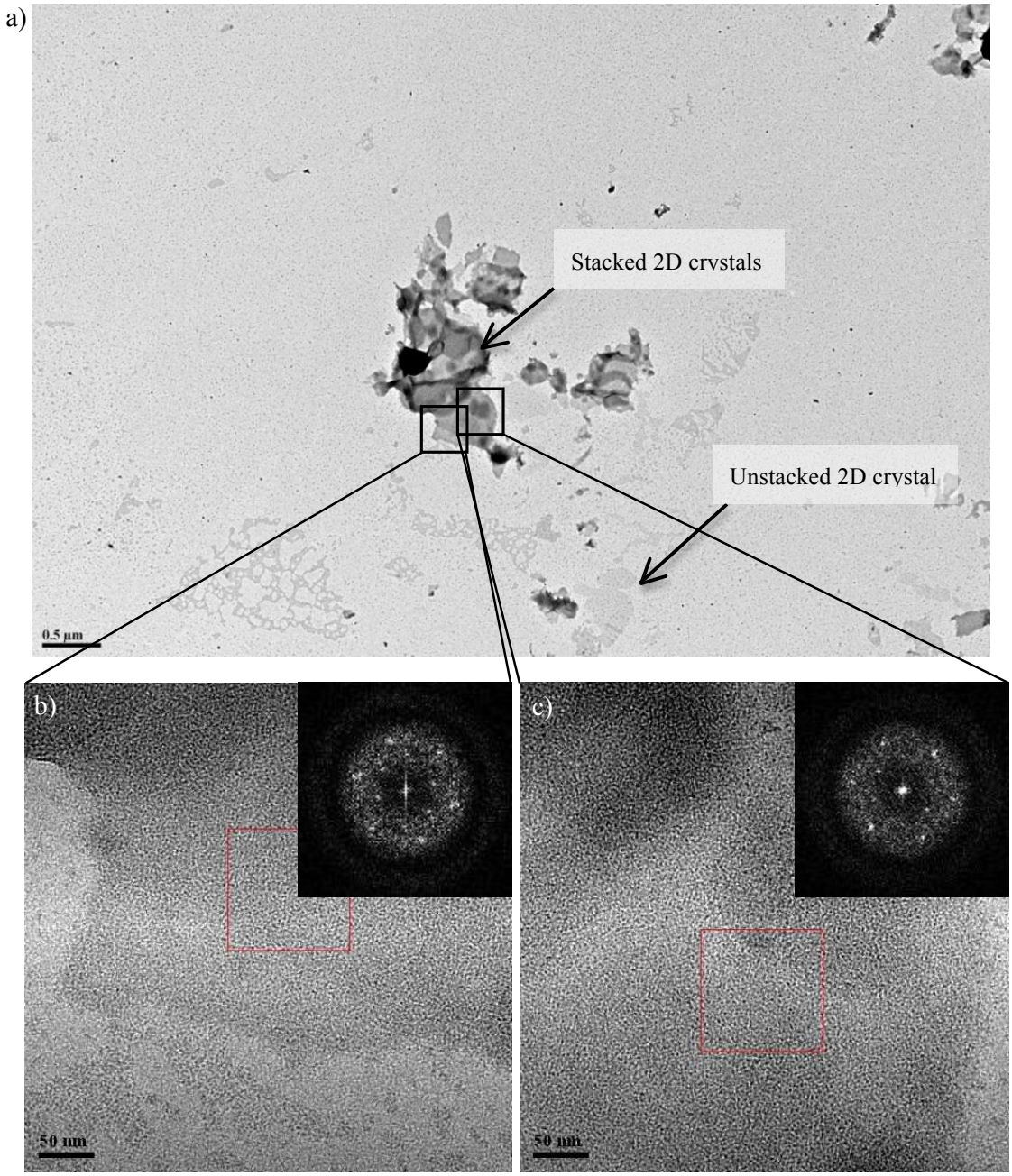

Figure 3.10. 2D stacked crystals of hLTC$_4$S mutant R104A. At a molar LPR of 15 stacked 2D crystals of mutant R104A, at a concentration of 0.21 mg/mL, were grown. a) Low-magnification micrograph of negatively stained hLTC$_4$S mutant R104A. Stacked sheets, 0.2 – 0.5 µm observed. b) and c) High-magnification micrograph of boxed areas in a) along with FFT analysis (inset) of boxed red area. Scale bar = 0.5 µm.

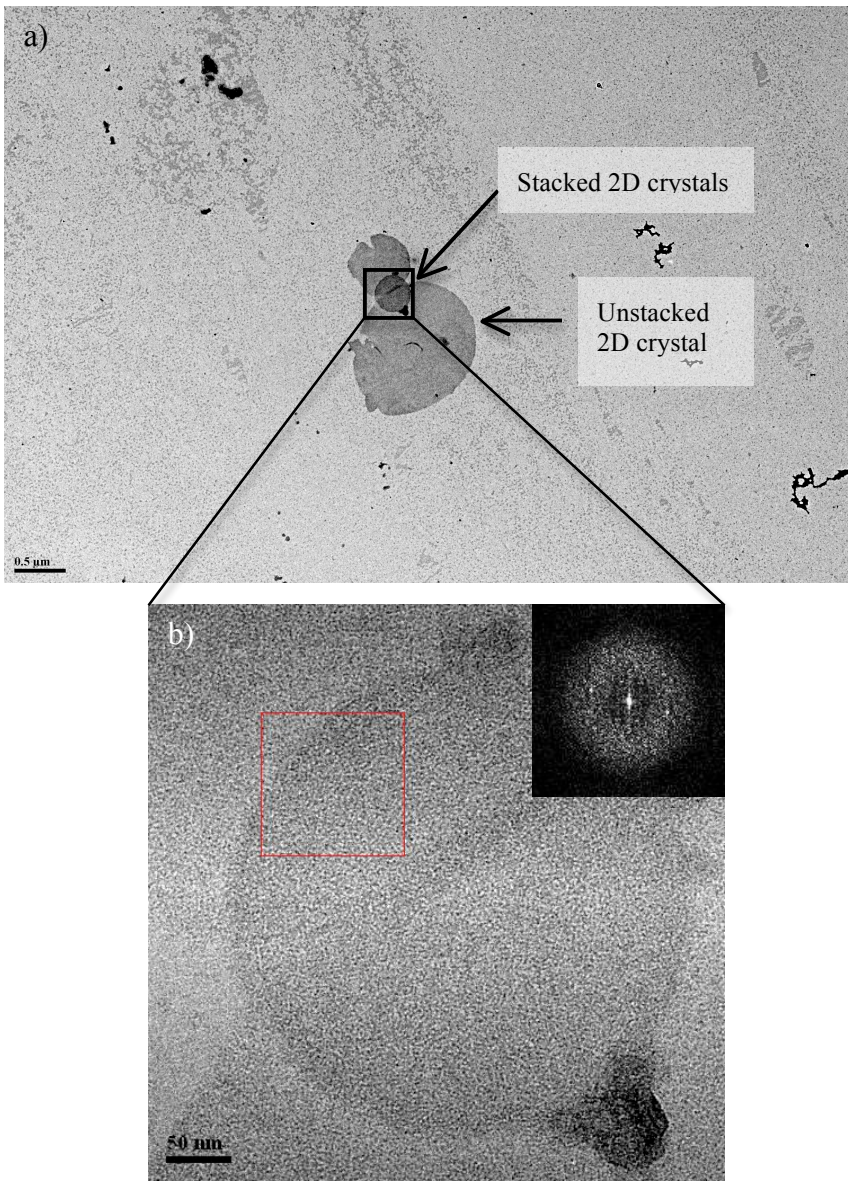

Figure 3.11. 2D crystal of hLTC$_4$S mutant R104A. At an LPR of 15, growth of unilamellar 2D crystals of mutant R104A were observed. a) Low-magnification micrograph of negatively stained hLTC$_4$S mutant R104A. Stacked sheets 0.2 – 0.7 µm in length were seen. b) and c) high-magnification micrograph of boxed areas in a) along with FFT analysis (inset) of boxed area (red). Scale bar = 0.5 µm.

Compared to previously reported data of $hTLC_4S$ WT, which formed well-ordered two-dimensional crystals at low LPRs, (Schmidt-Krey *et al.,* 2004 and Zhao *et al*., 2010) $hLTC_4S$ WT and mutant R104A is observed to crystallize at relatively high LPR values using a modified purification protocol. This may be due to efficient delipidation and removal of co-purified lipids during purification, thus requiring a larger amount of lipid for successful reconstitution. The identity of co-purified lipids can be assessed using 2D thin layer chromatography (TLC) where lipid molecules can be identified by comparison to commercially available pure lipid compounds (Christie, 1982). The presence of any remaining lipid molecules attached to $hLTC_4S$ might suggest their importance in structure and function of the enzyme. Identification of any co-purified lipids would provide insight into the degree of delipidation that was achieved after purification, and also would help to determine the amount of exogenous lipid that must be added for reconstitution.

As mentioned earlier, ionic strength plays a role in 2D crystallization trials. Increased ionic strength is characteristic of 3D crystallization trials, acting as a precipitant to increase hydrophilic interactions between the soluble domains of MPs. Small 2D crystals of LHC-II were obtained by dialysis against 200 mM KCl (Kühlbrandt, 1984), which is a high enough concentration of monovalent ions to charge surface amino acids and induce 2D crystal stacking (Kühlbrandt, 1992). $hLTC_4S$ was crystallized by dialysis against 50 mM KCl, which is typical for many MP 2D crystallization trials. Ionic strength may play a factor in the stacking of 2D crystals, as mono- and divalent cations screen surface charges allowing stacking to occur via non-polar interactions (Abeyrathne *et al.,* 2010). Another possible explanation for crystal stacking is the presence of α-helix V, which protrudes out of the membrane (Figure 3.2) (Zhao *et al*., 2010). Also, a C-terminal His_6-tag is attached to the end of helix V, which may present additional interactions between 2D membranes. If the fifth helix is to blame for crystal stacking it may be removed as it does not contain the amino acid residues critical for

substrate binding, although helix V may still be important for enzyme structure and function. Enzymatic activity of $hLTC_4S$, with removed helix V, should be confirmed prior to any crystallization attempts.

Upon the determination of successful conditions for 2D crystal formation with negative stain, the next step towards the 3D structure determination is electron cryo-microscopy of frozen-hydrated specimen. With this technique 2D crystals are left unstained and frozen in a layer of vitrified buffer that helps preserve the native structure of the MP for structure analysis. Negatively stained 2D crystals are limited in resolution by the grain size of the heavy metal stain. Frozen-hydrated specimens can produce greater details of the architecture of the enzyme because there is no stain to limit the resolution (Kühlbrandt, 1992).

3.4 CONCLUSIONS

Parameters for the 2D crystallization of $hLTC_4S$ mutant R104A, including LPR and time in dialysis variations, were investigated, based on previously published methods on the WT enzyme. Stacks and single layers of 2D sheets were observed after 3 – 8 days in dialysis at relatively high LPR values (LPR = 15), most likely due to the efficient removal of co-purified lipids. Fine-tuning of LPR values needs to be further investigated with focus on lowering LPR values to obtain well-ordered and large 2D crystals. Future directions for the R104A mutant enzyme include removal of helix 5, which protrudes into the solvent, and may be the cause of 2D crystal stacking.

Stacked 2D crystals are not desired for image processing and data collection by transmission electron microscopy, as tilting samples of thin, stacked crystals will not provide useful 3D data. Unstacked and large crystals will provide increasing amounts of structural detail. The unstacked crystals of mutant R104A can be used for future cryo-EM studies, because FFT analysis of negatively stained are limited in resolution due to stain grain size. Cryo-EM of these samples will usually reveal that these samples are highly ordered.

3.5 BIBLIOGRAPHY

Abeyrathne, P.D., Chami, M., Pantelic, R.S., Goldie, K.N., Stahlberg, H., 2010. Preparation of 2D crystals of Membrane Proteins for High-Resolution Electron Crystallography Data Collection. *Methods in Enzymology* 481 (10), 81001 - 81008.

Ago, H., Kanaoka, Y., Irikura, D., Lam, B.K., Shimamura, T., Austen, K.F., Miyano, M., 2007. Crystal structure of a human membrane protein involved in cysteinyl leukotriene biosynthesis. *Nature* 448 (7153), 609 - 612.

Appel, M., Hizlan, D., Vinothkumar, K.R., Ziegler, C., Kühlbrandt, W., 2009. Conformations of NhaA, the Na/H exchanger from Escherichia coli, in the pH-activated and ion-translocating states. *Journal of Molecular Biology* 386 (2), 351 - 365.

Boekema, E.J., Wynn, R.M., Malkin, R., 1990. The structure of spinach photosystem-I studied by electron microscopy. *Biochimica et Biophysica Acta* 1018, 49 – 56.

Christie, W., 1982. A simple procedure for rapid transmethylation of glycerolipids and chloesteryl esters. *Journal of Lipid Research* 23 (7), 1072 – 1075.

Dekker, J.P., Betts, S.D., Yocum, C.F., Boekema, E.J., 1990. Characterization by electron microscopy of isolated particles and two-dimensional crystals of the CP47-D1-D2-Cytochrome b-559 complex of photosystem II. *Biochemistry* 29 (13), 3220 – 3225.

Deisenhofer, J., Epp, O., Miki, K., Huber, R., Michel, H., 1985. Structure of the protein subunits in the photosynthetic reaction centre of Rhodopseudomonas viridis at 3 angstrom resolution. *Nature* 318 (6047), 618 – 624.

Gonen, T., Cheng, T., Sliz, P., Hiroaki, Y., Fujiyoshi, Y., Harrison, S.C., Walz, T., 2005. Lipid-protein interactions in double layered two-dimensional AQP0 crystals. *Nature* 438 (7068), 633 – 638.

Goswami, P., Paulino, C., Hizlan, D., Vonck, J., Yildiz, O., Kühlbrandt, W., 2011. Structure of the archael Na/H antiporter NhaP1 and functional role of transmembrane helix 1. *EMBO Journal* 30 (2), 439 – 449.

Grigorieff, N., Ceska, T.A., Downing, K.H., Baldwin, J.M., Henderson, R., 1996. Electron-crystallographic refinement of the structure of bacteriorhodopsin. *Journal of Molecular Biology* 259 (3), 393 – 421.

Gulik-Krzywicki, T., 1987. Monomer-oligomer equilibrium of bacteriorhodopsin in reconstituted proteoliposomes. *Journal of Biological Chemistry* 262 (32), 15580 – 15588.

Henderson, R. and Unwin, P.N.T., 1975. Three-dimensional model of purple membrane obtained by electron microscopy. *Nature* 257 (5521), 28 – 32.

Holm, P.J., Bhakat, P., Jegerschold, C., Gyobu, N., Mitsuoka, K., Fujiyoshi, Y., Morgenstern, R., Hebert, H., 2006. Structural basis for detoxification and oxidative stress protection in membranes. *Journal of Molecular Biology* 360 (5), 934 – 945.

Hovmöller, S., Slaughter, M., Berrman, J., Karlsson, B., Weiss, H., Leonard, K., 1983. Structural studies of cytochrome reductase. *Journal of Molecular Biology* 165 (2), 401 – 406.

Jakobsson, P.J., Morgenstern, R., Mancini, J., Ford-Hutchinson, A., Persson, B., 1999. Common structural features of MAPEG- A widespread superfamily of membrane associated proteins with highly divergent functions in eicosanoid and glutathione metabolism. *Protein Science* 8, 689 – 692.

Jegerschold, C., Pawelzik, S.C., Purhonen, P., Bhakat, P., Gheorghe, K.R., Gyobu, N., Mitsuoka, K., Morgenstern, R., Jakobsson, P.J., Hebert, H., 2008. Structural basis for induced formation of the inflammatory mediator prostaglandin E2. *Proc. Natl. Acad. Sci USA* 105, 11110 – 11115.

Karrasch, S., Typke, D., Walz, T., Miller, M., Tsiotis, G., Engel, A., 1996. Highly ordered two-dimensional crystals of photosystem I reaction center from Synecchoccus sp.: functional and structural analyses. *Journal of Molecular Biology* 262 (3), 336 – 348.

Kühlbrandt, W., 1984. Three-dimensional structure of the light-harvesting chlorophyll a/b-protein complex. *Nature* 307, 478 – 480.

Kühlbrandt, W., 1992. Two-dimensional crystallization of membrane proteins. *Quarterly Review of Biophysics* 25 (1), 1 – 49.

Kühlbrandt, W., 2012. Combining cryo-EM and x-ray crystallography to study membrane protein structure and function. Macromolecular Crystallography: Deciphering the Structure, Function and Dynamics of Biological Molecules. Ed. Maria Armenia Carronda and Ed. Paola Spadon. 1st. Dodrecht: Springer, 2012, 93 – 101.

Lam, B.K., Penrose, J.F., Freeman, G.J., Austen, K.F., 1994. Expression cloning of a cDNA for human leukotriene C4 synthase, an integral membrane protein conjugating reduced glutathione to leukotriene A4. *Proceedings of the National Academy of Sciences* 91 (16), 7663 – 7667.

Lam, B.K., Penrose, J.F., Xu, K., Baldasaro, M.H., Austen, K.F., 1997. Site-directed mutagenesis of human leukotriene C4 synthase. Journal of Biological Chemistry 272 (21), 13923 – 13928.

Mandal, A.K., Skoch, J., Bacskai, B.J., Hyman, B.T., Christmas, P., Miller, D., Yamin, T.T., Xu, S., Wisniewski, D., Evans, J.F., Soberman, R.J., 2004. The membrane organization of leukotriene synthesis. *Proc. Natl. Acad. Sci. USA* 101, 6587–6592.

Molina, D.M., Wetterholm, A., Kohl, A., McCarthy, A.A., Niegowski, D., Ohlson, E., Hammarberg, T., Eshaghi, S., Haeggerstrom, J.Z., Nordlund, P., 2007. Structural basis for synthesis of inflammatory mediators by human leukotriene c4 synthase. *Nature* 448 (7153), 613 – 617.

Mosser, G., 2001. Two-dimensional crystallogenesis of transmembrane proteins. *Micron* 32 (5), 517 – 540.

Newby, Z., O'Connell III, J.D., Gruswitz, F., Hays, F.A., Harries, W.E., Harwood, I.M., Ho, J.D., Stroud, R.M., 2009. A general protocol for the crystallization of membrane proteins for x-ray structural investigation. *Nature Protocols* 4 (5), 619 - 637.

Nicholson, D.W., Ali, A., Waillancourt, J.P., Calaycay, J.R., Mumford, R.A., Zamboni, R.J., Ford-Hutchinson, A.W., 1993. Purification to homogeneity and the N-terminal sequence of human leukotriene C4 synthase: A homodimeric glutathione S-transferase composed of 18 kDa subunits. *Proceedings of the National Academy of Sciences* 90 (5), 2015 - 2019.

Penrose, J.F., Gagnon, L., Goppelt-Struebe, M., Myers, P., Lam, B.K., Jack, R.M., Austen, K.F., Soberman, R.J., 1992. Purification of human leukotriene C4 synthase. *Proceedings of the National Academy of Sciences* 89 (23), 11603 – 11606.

Rémigy, H.-W., Caoujolle-Bert, D., Suda, K., Schenk, A., Chami, M., Engel, A., 2003. Membrane protein reconstitution and crystallization by controlled dilution. *FEBS Letters* 555, 160 – 169.

Ren, G., Cheng, A., Reddy, V., Melnyk, P., Mitra, A.K., 2000. Visualization of a water selective pore by electron crystallography in vitreous ice. *Proceedings of the National Academy of Sciences* 98 (4), 1398 – 1403.

Rinaldo-Matthis, A., Ahmad, S., Wetterholm, A., Lachmann, P., Morgenstern, R., Haeggstrom, J.Z., 2012. Pre-steady-state kinetic characterization of thiolate anion formation in human leukotriene c4 synthase. *Biochemistry* 51 (4), 848 – 856.

Saino, H., Ukita, Y., Ago, H., Irikura, D., Nisawa, A., Ueno, G., Yamamoto, M., Kanaoka, Y., Lam, B.K., Austen, K.F., Mirano, M., 2011a. The catalytic architechture of leukotriene c4 synthase with two arginine residues. *Journal of Biological Chemistry* 286 (18), 16392 – 16401.

Saino, H., Ago, H., Ukita, Y., Miyano, M., 2011b. Seleno-detergent MAD phasing of leukotriene c4 synthase in complex with dodecyl-B-D-selenomaltoside. *Structural Biology and Crystallization Communications* 67 (pt 12), 1666 – 1673.

Schmidt-Krey, I., Lundqvist, G., Morgenstern, R., Hebert, H., 1998. Parameters for the two-dimensional crystallization for the membrane protein microsomal glutathione transferase. *Journal of Structural Biology* 123 (2), 87 – 96.

Schmidt-Krey, I., Murata, K., Hirai, T., Mitsuoka, K., Cheng, U., Morgenstern, R., Fujiyoshi, Y., Hebert, H. the projection structure of the membrane protein microsomal glutathione transferase at 3 angstrom resolution as determined from two-dimensional hexagonal crystals. *Journal of Molecular Biology* 288, 243 – 253.

Schmidt-Krey, I., Mitsuoka, K., Hirai, T., Murata, K., Cheng, Y., Fujiyoshi, Y., Morgenstern, R., Hebert, H., 2000. The three-dimensional map of microsomal glutathione transferase 1 at 6 angstrom resolution. *EMBO Journal* 19 (23), 6311 – 6316.

Schmidt-Krey, I., Kanaoka, Y., Mills, D.J., Irikura, D., Haase, W., Lam, B.K., Austen, K.F., Kühlbrandt, W., 2004. Human leukotriene c4 synthase at 4.5 angstrom resolution in projection. *Structure* 12 (11), 2009 – 2014.

Schmidt-Krey, I., 2007. Electron crystallography of membrane proteins: Two-dimensional crystallization and screening by electron microscopy. *Methods* 41, 417–426.

Seddon, A.M., Curnow, P., Booth, P.D., 2004. Membrane proteins, lipids and detergents: not just a soap opera. *Biochimica et Biophysical Acta* 1666 (1 – 2), 105 – 117.

Signorell, G.A., Kaufmann, T.C., Kukulski, W., Engel, A., Remigy, H., 2006. Controlled 2D crystallization of membrane proteins using methyl-B-cyclodextrin. *Journal of Structural Biology* 157 (2), 321 – 328.

Stoeckenius, W., Lozier, R., Bogomolni, R.A., 1979. Bacteriorhodopsin and the purple membrane of halobacteria. *Biochim. Biophys. Acta* 505, 215 – 278.

Stokes, D.L. and Green, N.M., 1990. Three-dimensional crystals of Ca+2-ATPase from sarcoplasmic reticulum. *Biophysical Journal* 57 (1), 1 – 14.

Svartz, J., Blomgran, R., Hammarstrom, S., Soderstrom, M., 2003. Leukotriene C4 synthase homo-oligomers detected in living cells by bioluminescence resonance energy transfer. *Biochim. Bio- phys. Acta* 1633*,* 90–95.

Tsiotis, G., Walz, T., Spyridaki, A., Lustig, A., Engel, A., Ghanotakis, D., 1996. Tubular crystals of a photosystem II core complex. *Journal of Molecular Biology* 259 (2), 241 0 248.

Ubarretxena-Belandia, I. Baldwin, J.M., Schuldiner, S., Tate, C.G., 2003. Three-dimensional structure of the bacterial multidrug transporter EmrE shows it is an asymmetric homodimer. *EMBO Journal* 22 (23), 6175 -6181.

Ubarretxena-Belandia, I. and Stokes, D.L., 2010. Present and future of membrane protein structure determination by electron crystallography. *Advances in Protein Chemistry and Structural Biology* 81, 33 - 60.

Vinothkumar, K.R., Smits, S.H.J., Kühlbrandt, W., 2005. pH-induced structural change in a sodium/proton antiporter from Methanococcus jannashii. *EMBO Journal* 24 (15), 2720 – 2729.

White, S.H., 2009. Biophysical dissection of membrane proteins. *Nature* 459, 344 – 346.

Williams, K.A., 2000. Three-dimensional structure of the ion-coupled transport protein NhaA. *Nature* 403 (6765), 112 – 115.

Wingfield, P., Arad, T., Leonard, K., Weiss, H., 1979. Membrane crystals of ubiquinone:cytochrome C reductase from Neurospora mitochondria. *Nature* 280, 696 – 697.

Zhao, G.X., Johnson, M.C., Schnell, J.R., Kanaoka, Y., Haase, W., Irikura, D., Lam, B.K., Schmidt-Krey, I., 2010. Two-dimensional crystallization conditions human leukotriene c4 synthase requiring adjustment of a particularly large combination of specific parameters. *Journal of Structural Biology* 169 (3), 450 – 454.